Metabolic engineering of E. coli for improving mevalonate production to promote NADPH regeneration and enhance acetyl-CoA supply

Satowa, Daichi ; Fujiwara, Ryosuke ; Uchio, Shogo ; Nakano, Mariko ; Otomo, Chisako ; Hirata, Yuuki ; Matsumoto, Takuya ; Noda, Shuhei ;…

(Citation)
Biotechnology and Bioengineering,117(7):2153-2164

(Issue Date)
2020-07

(Resource Type)
journal article

(Version)
Accepted Manuscript

Metabolic engineering of *E. coli* for improving mevalonate production to promote NADPH regeneration and enhance acetyl-CoA supply

Daichi Satowa[1], Ryosuke Fujiwara[1], Shogo Uchio[1], Mariko Nakano[1], Chisako Otomo[1], Yuuki Hirata[1], Takuya Matsumoto[2], Shuhei Noda[3], Tsutomu Tanaka*[1] and Akihiko Kondo[3,4]

Running Title: Improved mevalonate production using *E. col*i

[1] Department of Chemical Science and Engineering, Graduate School of Engineering, Kobe University, 1-1 Rokkodai, Nada, Kobe 657-8501, Japan

[2] Department of Chemical Engineering, Osaka Prefecture University, 1-1 Gakuen-cho, Naka-ku, Sakai, Osaka, 599-8531, Japan.

[3] Center for Sustainable Resource Science, RIKEN, 1-7-22 Suehiro-cho, Tsurumi-ku, Yokohama, Kanagawa 230-0045, Japan

[4] Graduate School of Science, Technology and Innovation, Kobe University, 1-1 Rokkodai, Nada, Kobe 657-8501, Japan

* Corresponding author: Tsutomu Tanaka (tanaka@kitty.kobe-u.ac.jp)

Tel/Fax: +81-78-803-6202

e-mail: tanaka@kitty.kobe-u.ac.jp

Tsutomu Tanaka ORCID iD: 0000-0002-7397-7360

Shuhei Noda ORCID iD: 0000-0001-5430-1966

Ryosuke Fujiwara ORCID iD: 0000-0003-1549-1087

Akihiko Kondo ORCID iD: 0000-0003-1527-5288

Abstract

Microbial production of mevalonate from renewable feedstock is a promising and sustainable approach for the production of value-added chemicals. We describe the metabolic engineering of *Escherichia coli* to enhance mevalonate production from glucose and cellobiose. First, the mevalonate-producing pathway was introduced into *E. coli* and the expression of the gene *atoB*, which encodes the gene for acetoacetyl-CoA synthetase, was increased. Then, the deletion of the *pgi* gene, which encodes phosphoglucose isomerase, increased the NADPH/$NADP^+$ ratio in the cells but did not improve mevalonate production. Alternatively, to reduce flux toward the TCA cycle, *gltA*, which encodes citrate synthetase, was disrupted. The resultant strain, MGΔgltA-MV, increased levels of intracellular acetyl-CoA up to sevenfold higher than the wild-type strain. This strain produced 8.0 g/L of mevalonate from 20 g/L of glucose. We also engineered the sugar supply by displaying beta-glucosidase (BGL) on the cell surface. When cellobiose was used as carbon source, the strain lacking *gnd* displaying BGL efficiently consumed cellobiose and produced mevalonate at 5.7 g/L. The yield of mevalonate was 0.25 g/g glucose (1 g of cellobiose corresponds to 1.1 g of glucose). These results demonstrate the feasibility of producing mevalonate from cellobiose or cellooligosaccharides using an engineered *E. coli* strain.

Keywords

Escherichia coli, Mevalonate, Metabolic engineering, Beta-glucosidase

1. Introduction

Mevalonate is an important intermediate of the mevalonate pathway (MVA pathway), which plays a role in the production of isoprenoids (Pitera et al. 2007; Martin et al. 2003). The MVA pathway is present in various organisms including eukaryotes and some prokaryotes (Kuzuyama and Seto 2012). Mevalonate synthesis begins with acetyl-CoA. Acetoacetyl-CoA is synthesized from two molecules of acetyl-CoA by acetoacetyl-CoA synthase. Next, 3-hydroxy-3-methylglutaryl-CoA (HMG-CoA) synthase synthesizes HMG-CoA from acetoacetyl-CoA and acetyl-CoA. Finally, HMG-CoA is converted to mevalonate by HMG-CoA reductase (Figure 1a).

Various studies focused on producing mevalonate by fermentation have been conducted after mevalonate was discovered as a growth factor for *Lactobacillus heterohiochi* in 1956 (Cresson et al. 1956; Tamura et al. 2004). Tabata and Hashimoto introduced two genes, *mvaS* and *mvaE* from *Enterococcus faecalis* which expressed HMG-CoA synthase and HMG-CoA reductase, respectively, into *Escherichia coli*. The *E. coli* strain exhibited a high titer (47 g/L) within two days (Tabata and Hashimoto 2004). Xiong et al. tested several genes from various species using *E. coli* as a host for mevalonate production, and they determined that genes from *Lactobacillus casei* are most effective (Xiong et al. 2014). Wang et al. succeeded in producing mevalonate by

integrating genes involved with mevalonate synthesis genes into the chromosome of *Escherichia coli* using a constructed plasmid-free system (Wang et al. 2016). Masuda et al. improve mevalonate production by limiting nutrients in the medium and through cultivation at the stationary phase (Masuda et al. 2017). Nagai et al. also suggested that the Enter-Doudorff pathway (ED pathway) is more suitable for mevalonate production compared to the Embden-Meyerhof-Parnas Pathway (EMP pathway) according to the results of metabolic and thermodynamic analyses (Nagai et al. 2018). Wang et al. constructed the "EP-bifido pathway" by introducing the *fxpk* gene from *Bifidobacterium adolescentis* into *E. coli* to increase the supply of acetyl-CoA and produce a high yield (64.7 mol%) of mevalonate (Wang et al. 2018).

The biomass-derived fuels and chemicals has attracted much attention due to the possibility of a solutions of global warming and promoting bio-economy. Lignocellulosic biomass is abundant, cheep, and renewable feedstocks (Taha et al. 2016). However, it is difficult for most microorganisms to utilize lignocellulosic biomass directly, and the degradation of lignocellulose takes high cost and multiple process. A synergistic combination of the cellulolytic enzymes endoglucanase (EG), cellobiohydrolase (CBH), and β-glucosidase (BGL) can be useful for cellulose decomposition. EG and CBH can produce cellobiose and some cellooligosaccharides

from cellulose. Then cellobiose can be hydrolyzed to glucose by BGL. BGL also enhances cellulose hydrolysis by avoiding inhibition of EG and CBH activities caused by cellobiose (Bayer et al. 2007). However, the addition of large amounts of BGL is required for cellulose hydrolysis, due to the low levels of BGL in commercially-available cellulases mixture (Sukumaran et al. 2010). To date, only a few studies on the chemicals production such as isopropanol (Soma et al. 2012), cadaverine (Ikeda et al. 2013), isobutanol (Desai et al. 2014) directly from cellobiose or cello-oligosaccharides by using *E. coli* have been reported, while no reports of the production of mevalonate from cellobiose using *E. coli*. The use of BGL-expressing *E. coli* has the potential to reduce cellulases requirements, which will lead to significant cost reduction of cellulosic biomass-derived chemicals production.

Most studies have considered the heterologous pathway and culture conditions used for mevalonate synthesis. Here we focus on the engineering of *E. coli* to enhance mevalonate production via targeted improvements in the pools of NADPH and acetyl-CoA because 2 mol of NADPH and 3 mol of acetyl-CoA are consumed when1 mol of mevalonate is produced. After establishing an initial expression system, metabolic pathways were engineered to improve mevalonate biosynthesis. First, the glycolysis pathway was engineered to compensate for NADPH by promoting carbon

flux toward the ED pathway or the pentose-phosphate pathway (PP pathway) instead of the EMP pathway. Second, the tricarboxylic acid cycle (TCA cycle) was engineered to increase the supply of acetyl-CoA for the MVA pathway. Further, we demonstrate the feasibility of direct mevalonate production using cellobiose as a carbon source.

2. Materials and Methods

2.1 Strains and plasmid construction, medium, culture conditions

The strains and plasmids used in this study are listed in Table 1. *E. coli* NovaBlue competent cells (Novagen, Cambridge, MA, USA) were used for gene cloning. Polymerase chain reaction (PCR) was performed using KOD FX (TOYOBO, Osaka, Japan). Custom DNA oligonucleotide primers were obtained from Invitrogen Custom DNA Oligos (Thermo Fisher Scientific, Tokyo, Japan). Codon-optimized genes fragments (*mvaS* and *mvaE,* both from *E. faecalis*) were provided by the Invitrogen GeneArt Gene Synthesis service (Thermo Fisher Scientific, Tokyo, Japan). Details of plasmid and strain construction, medium, and culture conditions are described in Supporting information. The sequences of primers and genes fragments are shown in Table S1 and Table S2, respectively.

2.2 Quantification of Acetyl-CoA and NADPH and analytical methods

Preparation of samples for the analysis of Acetyl-CoA and NADPH was conducted according to the following procedures. *E. coli* strains were precultured in 5 mL LB medium overnight at 37 °C. The preculture medium was seeded to 5 mL M9Y medium at an initial OD_{600} of 0.05. After 4 h of cultivation, 4 mL of cultured cells were centrifuged at 3500 g for 5 min. Extraction buffer (methanol: chloroform = 7:3) was added to cells and incubated at 1000 rpm, 4 °C overnight. The supernatant was centrifuged at 13000 g for 5 min and evaporated. The evaporated samples were analyzed using the Enzychrom $NADP^+$/NADPH Assay Kit ECNP-100 (BioAssay Systems, Hayward, USA) and PicoProbe Acetyl-CoA Fluorometric Assay Kit (BioVision Incorporated, Milpitas, USA), according to the manufacturers' procedures.

2.3 Medium

M9Y medium was used for mevalonate production in 5 mL test tube-scale cultures. M9Y medium was comprised of M9 minimal medium supplemented with 0.5 % yeast extract, 0.008 g/L D-(+)-biotin, 0.2 g/L citrate, 0.008 g/L nicotinic acid, 0.032 g/L, pyridoxine and 1 mL/L trace metal solution. M9 minimal medium contains (per liter) 20 g glucose or cellobiose, 0.5 g NaCl, 6.7 g Na2HPO4, 3 g KH2PO4, 1 g NH4Cl, 246

mg MgSO4·7H2O, 14.7 mg CaCl2·2H2O, 2.78 mg FeSO4·7H2O, and 10 mg thiamine hydrochloride. When needed, ampicillin (100 mg/L) was added to the initial medium.

2.4 Culture Conditions

To promote mevalonate fermentation from glucose and cellobiose, metabolically-engineered strains were precultured in 5 mL LB medium overnight at 37 °C. The preculture medium was seeded to 5 mL M9Y medium in a 15 mL test tube at an initial optical density at 600 nm (OD600) of 0.05. After 3 h of cultivation, isopropyl β-D-1-thiogalactopyranoside was added to a final concentration of 0.1 mM. The tube-scale cultures were incubated at 37 °C with shaking at 220 rpm.

2.5 Analytical Methods

HCl (50 µL) was added to 300 µL of cultured cells and incubated at 60 °C with shaking at 1000 rpm for lactonization. After 30 min, mevalonolactone was extracted with 350 µL of ethyl acetate containing beta-caryophyllene as an internal standard. Cell growth was determined by measuring the OD at 600 nm (OD600) on a UVmini-1240 spectrophotometer (Shimadzu Corporation, Kyoto, Japan). Extracted mevalonolactone was analyzed by gas chromatography (GC) using a GC-2025

chromatograph (Shimadzu Corporation, Kyoto, Japan) equipped with an SH-stabilwax (Length 30 m, Diameter 0.25 mm, Film 0.25 μm). Glucose and cellobiose were analyzed using a Prominence high-performance liquid chromatography (HPLC) System (Shimadzu Corporation, Kyoto, Japan) equipped with a Shodex SUGAR KS-801 column (6 μm, 300 mm × 8.0 mm, L × I.D., SHOWA DENKO, Tokyo, Japan). Water was used as the mobile phase with a flow rate of 0.8 mL/min, and the column was maintained at 50 °C. The HPLC profile was monitored using a refractive index detector.

3. Results

3.1 Reconstruction of mevalonate biosynthetic pathway in *E. coli* MG1655

The pathway for mevalonate synthesis is shown in Figure 1a. We selected *mvaS* and *mvaE* from *E. faecalis,* which code for HMG-CoA synthase and HMG-CoA reductase, respectively (Hedl et al. 2002; Tabata and Hashimoto 2004). Four types of plasmids were constructed for mevalonate production and introduced in *E. coli* MG1655 strain (Figure 1b). A plasmid pMeES contains the *mvaE* and *mvaS* genes under the control of the Trc promoter. To enhance the utility of acetyl-CoA for mevalonate synthesis, co-expression of endogenous acetoacetyl-CoA synthase using

the gene *atoB* is another option. The plasmid pMeESA contains *mvaE-mvaS-atoB* while the plasmid pMeAES contains *atoB-mvaE-mvaS*. We also constructed the plasmid pZA-AES, which expresses *atoB*, *mvaE,* and *mvaS* under the control of the lac promoter. Figure 1c shows the mevalonate titer from a concentration of 20 g/L of glucose in the M9Y medium after 48 h of cultivation. A small amount of mevalonate (0.25 g/L) was produced by the strain harboring pMeES. Meanwhile, the strains harboring pMeESA or pMeAES had improved mevalonate production compared to pMeES, and the strain harboring pMeAES exhibited a high titer of mevalonate (5.25 g/L). The lac promoter is another candidate for the overexpression of genes involved with mevalonate synthesis. However, the strain harboring pZA-AES produced only a small quantity of mevalonate (0.27 g/L). Although both promoters are strong, the copy number of pZA-AES (p15A Ori) lower than that of pMeAES (ColE1 Ori), which caused the little amount of mevalonate production. These results show that it is important to pull acetyl-CoA into the MVA pathway by increasing the expression of *atoB*. Therefore, we used the plasmid pMeAES in subsequent experiments.

3.2 Improvements of NADPH regeneration by gene disruption

An NADPH supply is necessary for mevalonate production because the last

step of mevalonate production that is catalyzed by *mvaE* requires the consumption of 2 mol NADPH per mol of mevalonate. NADPH is mainly generated through the PP pathway. To increase carbon flux into the PP pathway, we focused on three genes, *pgi* (phosphoglucose isomerase), *pfkA* (ATP-dependent phosphofructokinase), and *pfkB* (ATP-dependent phosphofructokinase isozyme 2). The *pgi* gene encodes the enzyme involved with the first step of the EMP pathway, which has been used to increase carbon flux through the PP pathway (Lin et al. 2014). The *pfk* gene encodes an enzyme that catalyzes the phosphorylation of fructose-6-phosphate to fructose-1,6-biphosphate, which is a key step of the major glycolytic pathway (Frankel et al. 1975). In addition, *E. coli* has two isoenzymes for phosphofructokinases: *pfkA* and *pfkB*. The *pfkA* gene has been reported to contribute 90% of the phosphofructokinase activity while *pfkB* is the minor enzyme that contributes to 5%–10% of overall phosphofructokinase activity (Vinopal et al. 1975). In another study (Siedler et al. 2011), *pfkA* mutants showed 23 % of wild-type activity while *pfkB* mutants showed 78 % of wild-type activity; the double mutant exhibited 27 % of wild-type activity.

Here, we constructed *pgi*, *pfkA,* or *pfkB* gene-deficient strains and evaluated the NADPH/$NADP^+$ ratio of each strain (Figure 2a). As expected, the NADPH/$NADP^+$ ratio of MGΔpgi is about sevenfold higher than that of the wild-type followed by a

threefold improvement in the MGΔpfkA strain. In the *pfkB*-deficient strain, the NADPH/$NADP^+$ ratio was slightly decreased compared to the ratio in the wild-type strain, which corresponded to the findings in a previous report (Siedler et al. 2011).

The mevalonate production of the strains harboring pMeAES after 48 h of cultivation is shown in Figure 2b. Although the cellular growth of these strains was increased (Figure 2c), the mevalonate titer of MGΔpgi-MV (3.49 g/L) and MGΔpfkA-MV (3.17 g/L) were decreased compared to wild-type (5.25 g/L). The mevalonate titer of the *pfkB*-deficient strain MGΔpfkB-MV (4.64 g/L) was slightly lower than the titer of the wild-type strain. These results demonstrated that the NADPH supply was not a rate-limiting step in mevalonate production.

We also constructed a *gnd*-deficient strain (MGΔgnd) to function as a branch point between the ED pathway and the PP pathway. Enhancing the ED pathway is a promising approach to increase mevalonate production (Nagai et al. 2018). The titer of mevalonate using the *gnd*-deficient strain MGΔgnd-MV was only slightly increased (5.49 g/L) compared to wild-type production (Figure 2b), which corresponds to the previous reports. However, the NADPH/$NADP^+$ ratio of MGΔgnd was not increased compared to the wild-type (Figure 2a). These results also showed that NADPH regeneration was not a key priority for producing mevalonate.

3.3 Enhancement of acetyl-CoA supply by gene disruption

Acetyl-CoA is a precursor of TCA cycle, competing with mevalonate production. Hence, we focused on the genes *ppc* and *gltA*, which encode phosphoenolpyruvate carboxylase and citrate synthase, respectively. Phosphoenolpyruvate carboxylase produces oxaloacetate from phosphoenolpyruvate as an anaplerotic reaction. The deletion of the *ppc* gene reduces the oxaloacetate supply and weakens the TCA cycle flux. Citrate synthetase catalyzes the condensation reaction of acetyl-CoA and oxaloacetate to citrate, which is important for entry into the TCA cycle and a key pace making step for bacterial growth. The deletion of *gltA* has rarely been employed in metabolic engineering because of its negative impact on bacterial growth (Heo et al. 2017). Glyoxylate shunt is another pathway that consumes acetyl-CoA; genes involved with this pathway encode malate synthetase (*aceB*) and isocitrate synthetase (*aceA*). We constructed *ppc*, *gltA,* or *aceBA* gene-deficient strains and measured the levels of acetyl-CoA among these strains (Figure 3a). The acetyl-coA levels of MGΔgltA was approximately twice that of the wild-type strain, followed by MGΔppc (1.25-fold higher). MGΔaceBA showed almost the same levels of acetyl-CoA as the wild- type strain. The double-deletion variants MGΔppcΔaceBA did not

increase levels of acetyl-CoA. The other strain MGΔppcΔgltA improved the acetyl-CoA levels by up to 150% compared to wild-type.

The mevalonate production of the strains harboring pMeAES after 48 h of cultivation is shown in Figure 3b. Contrary to Figure 2, the cellular growth of these strains was decreased (Fig. 3c). The strains MGΔgltA-Mv (7.19 g/L) and MGΔppc-Mv (7.04 g/L) produced high quantities of mevalonate compared to wild-type cells (5.25 g/L). MGΔaceBA-Mv produced 4.58 g/L of mevalonate, which was lower than that of MG1655-MV. The double-knockout strain MGΔppcΔgltA-Mv produced 5.87 g/L of mevalonate, which was slightly lower than MGΔgltA-Mv. MGΔppcΔaceBA produced 6.95 g/L of mevalonate, which was approximately the same as that of MGΔppc-Mv. These results showed that enhancing the supply of acetyl-CoA pool is more effective for mevalonate production than regenerating NADPH.

We also evaluated the levels of acetyl-CoA in MGΔgnd (Figure 3a), which were approximately equivalent to levels in the wild-type strain. The deletion of *gnd* did not cause the accumulation of acetyl-CoA nor NADPH (Figure 2a), which corresponded to the previous report (Jiao et al. 2003). The double-deletion mutant, MGΔgndΔgltA, did not produce higher levels of mevalonate compared to the wild-type (Figure 3b). Furthermore, we additionally introduced pZA-AES into MGΔgltA-

Mv, but this only led to a slight increase in mevalonate production (Figure 3b). We also introduced pZA-XPK into MGΔgltA-Mv according to previous report (Wang et al. 2018). However, pZA-XPK had no positive effect to MGΔgltA-Mv after 66h cultivation (data not shown). These results suggest that the levels of enzymes are sufficient for mevalonate production.

3.4 Culture profiles of mevalonate-producing strains

The time-dependent mevalonate production among strains exhibiting a high mevalonate titer in Figure 2 and Figure 3 was evaluated. MG1655-Mv, MGΔgnd-Mv, MGΔppc-Mv, MGΔppcΔaceBA-Mv, MGΔgltA-Mv, MGΔgltAΔppc-Mv were cultivated in M9Y medium containing 20 g/L of glucose. Mevalonate production, cellular growth rates, and rates of sugar consumption are shown in Figure 4. The titer of MG1655-Mv after 24 h of cultivation reached 6.15 g/L, then gradually decreased (Figure 4a). Other strains also showed similar culture profiles. The cell growth of MG1655-Mv and MGΔgnd-Mv was higher than other strains and the OD_{600} was equal to 11 after 24 h of cultivation (Figure 4b). However, the cellular growth of *ppc* or *gltA*-deficient strains were lower than that of MG1655-Mv. MG1655-Mv consumed almost all of the glucose after 10 h in culture (Figure 4c) and MGΔgnd-Mv consumed 15 g/L

of glucose after 10 h. Alternatively, the other four strains consumed glucose at a slower rate compared to MG1655-Mv and MGΔgnd-Mv (Figure 4c). After 12 h of cultivation, the cell growth of these strains stopped but the residual glucose was gradually consumed, which might lead to higher mevalonate production.

3.5 Mevalonate production from cellobiose as a carbon source

To produce mevalonate from cellobiose as a carbon source, we constructed a plasmid that co-expressed BGL with genes involved in the mevalonate-producing pathway. We employed cell surface display for BGL expression, which is a powerful tool for improving the activity of a displayed protein (Lee et al. 2003; Tanaka et al. 2011, 2014). The strains harboring pMeAES-BGL were cultured with 20 g/L of cellobiose as a sole carbon source. The rate of mevalonate production after 48 h is shown in Figure 5a. The strain MG1655-MvBGL produced 1.75 g/L of mevalonate from cellobiose, which is lower than the rate of production from glucose (5.25 g/L; Figure 2b). The MGΔgnd-MvBGL strain showed the highest mevalonate titer from glucose (5.49 g/L) produced 5.27 g/L of mevalonate from cellobiose. Although MGΔppc-Mv and MGΔgltA-Mv showed high mevalonate titers from glucose, MGΔppc-MvBGL and MGΔgltA-MvBGL produced nearly equal quantities of

mevalonate from cellobiose as MG1655-MvBGL. However, MGΔppcΔaceBA-MvBGL produced 5.03 g/L of mevalonate from cellobiose, which was the same as MGΔgnd-MvBGL. A triple-deletion strain, MGΔppcΔaceBAΔgnd-MvBGL, did not improve the mevalonate titer (4.52 g/L). The cellular growth of these strains is shown in Figure 5b. All strains showed reduced cellular growth compared to MG1655-MvBGL.

The time-dependent rates of mevalonate production from cellobiose were also evaluated. MG1655-MvBGL, MGΔgnd-MvBGL, MGΔgltA-MvBGL, MGΔppcΔaceBA-MvBGL, MGΔgltAΔppc-MvBGL were cultivated in M9Y medium containing 20 g/L of cellobiose. Rates of mevalonate production, cellular growth, and sugar consumption are shown in Figure 6. The titer of MG1655-MvBGL after 24 h cultivation reached 1.7 g/L (Figure 6a). MGΔgnd-MvBGL produced the highest amount of mevalonate (5.7 g/L) after 24 h of cultivation, followed by MGΔppcΔaceBA-MvBGL (5.0 g/L) after 48 h of cultivation. MG1655-MvBGL showed the highest rate of cellular growth among these strains followed by MGΔgnd-MvBGL (Figure 6b). Cellobiose was consumed after 24 h of cultivation. Glucose levels detected in the culture medium are shown in Figure 6d. In the case of MGΔgnd-MvBGL, only a small amount of glucose was detected (0.8 g/L) after 10 h of

cultivation, which suggests that the hydrolysis of cellobiose by BGL was not a rate-limiting step. On the other hand, 3.8 g/L of glucose was detected when MG1655-MvBGL was used, and 8.3 g/L of glucose was detected after 24 h of cultivation when MGΔppcΔaceBA-MvBGL was used. MGΔgltA-MvBGL produced almost the same amount of mevalonate as MG1655-MvBGL. Rates of cellular growth and cellobiose consumption for MGΔgltA-MvBGL were poor (Figures 6b, 6c). The acetyl-CoA level after 8 h cultivation from cellobiose was evaluated. MGΔgnd-MvBGL and MGΔgltA-MvBGL increased the acetyl-CoA level 1.35- and 1.56-fold, respectively, compared to MG1655-MvBGL (Fig. 6e). MGΔgnd-MvBGL and MGΔgltA-MvBGL produced 0.67 g/L and 0.91 g/L mevalonate, respectively (Fig. 6f).

4. Discussion

One of the key elements for the efficient production of mevalonate is the availability of intracellular NADPH as a cofactor. One approach is to replace an NAD(+)-dependent enzyme with an NADP(+)-dependent enzyme to redirect flux through the NADPH-generating PP pathway (Wang et al. 2013). Transhydrogenase PntAB overexpression increased NADPH reduction and improved the production of 3-hydroxypropionic acid, shikimic acid and Agmatine (Rathnasingh et al. 2012; Cui et

al. 2014; Xu and Zhang 2019). Here, we focused on enhancing PP pathway flux by deleting *pgi*, *pfkA,* and *pfkB*. The NADPH supply increased in the *pgi*-deficient strain and the *pfkA*-deficient strain (Figure 2a), which corresponds to previous reports (Siedler et al. 2011). However, the mevalonate titer of these strains was decreased compared to wild-type (Figure 2b), suggesting the NADPH supply was sufficient for mevalonate production. A *pfkB*-deficient strain exhibited almost the same NADPH/$NADP^+$ ratio as the wild-type strain because more than 90% of the phosphofructokinase activity in *E. coli* is carried by PfkA (Kotlarz et al. 1975). The cellular growth of *pgi*- or *pfkA*-deficient strain s was improved (Figure 2c) due to the accumulation of the anabolic redox cofactor NADPH (Cabulong et al. 2019).

Acetyl-CoA is involved in various biological processes and it serves as a platform chemical for producing various high-value products, such as 1-butanol (Dong et al. 2017; Ohtake et al. 2017), 3- hydroxypropionate (Liu et al. 2017; Cheng et al. 2016), polyhydroxyalkanoates (Zheng et al. 2017) and isoprenoids. Isoprenoids may be used for flavorings, biofuels, pharmaceuticals, vitamins (Ward et al. 2018; Wang et al. 2017). Acetyl-CoA is the most important precursor for mevalonate production. Blocking pathways that catabolize acetyl-CoA is an effective approach for obtaining acetyl-CoA derived compounds (Wu and Eiteman 2016; Dong et al. 2017). Acetate

formation is another pathway to reduce the supply of acetyl-CoA (Parimi et al. 2017; Saini et al. 2014; Kim et al. 2016. Acetyl-CoA is metabolized by phosphate acetyltransferase, which is encoded by *pta*, and the resultant product (acetyl-phosphate) is converted to acetate by acetate kinase (*ackA*) Pyruvate dehydrogenase (*poxB*) produces acetate from pyruvate, a precursor of acetyl-CoA. Only small amounts of acetate as by-products produced less than 1 g/L after MGΔgnd-Mv cultivation (Supporting Figure S1), suggesting that deleting the acetate-producing pathway had less of an effect on mevalonate accumulation.

Reducing the TCA cycle flux is effective for promoting acetyl-CoA accumulation. For example, genetic toggle switches could be used to alter the expression state between two different genes (Soma et al. 2014). Regulation of metabolic flux allows for switching the intracellular metabolism from the bacterial growth phase to the bio-production phase. Although switch-based metabolic controls could be applied to synthetic metabolic pathways while minimizing the negative effects on bacterial growth and cell maintenance, fine-tuning of the switch mechanism, which includes optimizing the timing of the inducer, is required (Soma et al. 2014; 2017). Alternatively, the deletion of *gltA* caused the accumulation of acetyl-CoA and increased citramalate production (Wu and Eiteman 2016, Parimi et al. 2017). In this

study, we demonstrated that *gltA* or *ppc* deletion had positive effects on mevalonate production (Figure 3) by reducing flux toward the TCA cycle (De Maeseneire et al. 2006; Chemler JA et al. 2010). The deletion of *ppc* also reduced the activity of isocitrate dehydrogenase (Peng et al. 2004), which catalyzes the entry reaction for the glyoxylate shunt. Glyoxylate shunt deficiency is also improved by the accumulation of acetyl-CoA (Figure 3a), but in this case, cellular growth was increased instead of mevalonate production (Figure 3c). The NADPH/$NADP^+$ ratios of *gltA* or *ppc*-deficient strains did not improve (data not shown), which suggests that acetyl-CoA accumulation is the main contributing factor toward mevalonate production (Figure 3).

When cellobiose was used as the sole carbon source, the MGΔgnd-MvBGL strain produced 5.7 g/L of mevalonate after 24 h from 20 g/L of cellobiose (Figure 6). This rate of production corresponds to a yield of 0.25 g mevalonate/g glucose (1 g of cellobiose corresponds to 1.1 g of glucose), which is slightly lower than the rate of mevalonate production obtained from glucose (0.31 g mevalonate/g glucose; Figure 4). Cellular growth using cellobiose as a carbon source was slower than that of glucose, and cellobiose was completely hydrolyzed by 24 h. However, free glucose was observed in the culture medium between 12 h and 48 h, thus indicating that the BGL-based conversion of cellobiose into glucose was enough and an improvement of

glucose uptake requires for enhancing mevalonate production. The acetyl-CoA levels of MGΔgltA-MvBGL was higher than MGΔgnd-MvBGL (Figure 6e), however, mevalonate production was decreased due to the reduction of cell growth (Figure 6b). While the addition of pyruvate helped recover the cell growth of MGΔgltA-MvBGL in cellobiose culture, mevalonate production did not improve (Supporting Figure S2). These results suggest the shortage of pyruvate may be partially responsible for the cell growth in MGΔgltA-MvBGL.

In the case of MGΔgnd-MvBGL, this strain produced mevalonate from cellobiose at almost the rate as when it used glucose as a carbon source. A gene *gnd* knockout generally causes a redirection of carbon flux from the PP pathway to the ED pathway, which supplies pyruvate. The enhanced anaplerotic pathway catalyzed by malic enzyme was accompanied by the up-regulation of phosphoenolpyruvate carboxylase and the down-regulation of phosphoenolpyruvate carboxykinase (Jiao et al. 2003). When cellobiose was used as a carbon source, MG1655-MvBGL produced large amounts of acetate as by-products than MG1655-Mv from glucose (Supporting Figure S1). On the other hand, MGΔgnd-MvBGL produced no acetate from cellobiose. It causes that MGΔgnd-MvBGL produced almost same level of mevalonate from cellobiose as that of MGΔgnd-Mv from glucose.

In conclusion, this *E. coli* strain was metabolically engineered for enhanced mevalonate production from glucose and cellobiose with metabolic pathways. This study contributes the developing an economically feasible and sustainable process for mevalonate production.

Acknowledgments

This work was supported by the JST-Mirai Program (Grant Number JPMJMI17EI), Japan (to S.N. and T.T.), the Japan Society for the Promotion of Science (JSPS) Grant-in-Aid for Scientific Research (B) (Grant Number 19H02526), Japan (to T.T.). The authors would like to thank Enago (www.enago.jp) for the English language review.

Conflicts of interest

The authors declare that there are no conflicts of interest.

References

Bayer, E.A., Lamed, R., & Himmel M.E. (2007). The potential of cellulases and cellulosomes for cellulosic waste management. *Current Opinion in Biotechnology*, *18*, 237-245. doi:10.1016/j.copbio.2007.04.004

Cabulong, R.B., Valdehuesa, K.N.G., Bañares, A.B., Ramos, K.R.M., Nisola, G.M., Lee, W.K., & Chung, W.J. (2019). Improved cell growth and biosynthesis of glycolic acid by overexpression of membrane-bound pyridine nucleotide transhydrogenase. *Journal of Industrial Microbiology and Biotechnology, 46,* 159-169. doi: 10.1007/s10295-018-2117-2

Chemler, J.A., Fowler, Z.L., McHugh, K.P., & Koffas, M.A. (2010). Improving NADPH availability for natural product biosynthesis in *Escherichia coli* by metabolic engineering. *Metabolic Engineering, 12,* 96-104. doi: 10.1016/j.ymben.2009.07.003.

Cresson, E.L., Folkers, K., Hoffman, C.H., Mavrae, G.D., Skeggs, H.R., Wolf, D.E., & Wright, L.D. (1956). Discovery of a new acetate-replacing factor. *Journal of*

Bacteriology, 72, 519-524.

Cheng, Z., Jiang, J., Wu, H., Li, Z., & Ye, Q. (2016). Enhanced production of 3-hydroxypropionic acid from glucose via malonyl-CoA pathway by engineered *Escherichia coli*. *Bioresource Technology, 200,* 897-904. doi: 10.1016/j.biortech.2015.10.107

Cui, Y.Y., Ling, C., Zhang, Y.Y., Huang, J., & Liu, J.Z. (2014). Production of shikimic acid from *Escherichia coli* through chemically inducible chromosomal evolution and cofactor metabolic engineering. *Microbial Cell Factories, 13*, 21. doi: 10.1186/1475-2859-13-21

De Maeseneire, S.L., De Mey, M., Vandedrinck, S., & Vandamme, E.J. (2006). Metabolic characterization of *E. coli* citrate synthase and phosphoenolpyruvate carboxylase mutants in aerobic cultures. *Biotechnology Letters, 23*, 1945-1953 doi: 10.1007/s10529-006-9182-8

Desai, S.H., Rabinovitch-Deere, C.A., Tashiro, Y., & Atsumi, S. (2014). Isobutanol

production from cellobiose in *Escherichia coli*. *Applied Microbiology and Biotechnology, 98*, 3727-3736. doi: 10.1007/s00253-013-5504-7.

Dong, H., Zhao, C., Zhang, T., Zhu, H., Lin, Z., Tao, W., Zhang, Y., & Li, Y. (2017). A systematically chromosomally engineered *Escherichia coli* efficiently produces butanol. *Metabolic Engineering, 44*, 284-292. doi: 10.1016/j.ymben.2017.10.014.

Fraenkel, D.G., Kotlarz, D., & Buc, H. (1975) Two fructose 6-phosphate kinase activities in *Escherichia coli*. *Journal of Biological Chemistry, 248*, 4865-4866.

Hedl, M., Sutherlin, A., Wilding, E.I., Mazzulla, M., McDevitt, D., Lane, P., Burgner, J.W. 2nd., Lehnbeuter, K.R., Stauffacher, C.V., Gwynn, M.N., & Rodwell, V.W. (2002). *Enterococcus faecalis* acetoacetyl-coenzyme A thiolase/3-hydroxy-3-methylglutaryl-coenzyme A reductase, a dual-function protein of isopentenyl diphosphate biosynthesis. *Journal of Bacteriology, 184*, 2116-2122 doi:10.1128/jb.184.8.2116-2122.2002

Heo, M.J., Jung, H.M., Um, J., Lee, S.W., & Oh, M.K. (2017). Controlling Citrate Synthase Expression by CRISPR/Cas9 Genome Editing for n-Butanol Production in *Escherichia coli*. *ACS Synthetic Biology, 17(6)*, 182-189. doi: 10.1021/acssynbio.6b00134

Ikeda, N., Miyamoto, M., Adachi, N., Nakano, M., Tanaka, T., & Kondo, A. (2013). Direct cadaverine production from cellobiose using β-glucosidase displaying *Escherichia coli*. *AMB Express, 3,* 67. doi: 10.1186/2191-0855-3-67

Jiang, Y., Chen, B., Duan, C., Sun, B., Yang, J., & Yang, S. (2015). Multigene editing in the *Escherichia coli* genome via the CRISPR-Cas9 system. *Applied and Environmental Microbiology, 8*1, 2506-2514. doi: 10.1128/AEM.04023-14

Jiao, Z., Baba, T., Mori, H., & Shimizu, K. (2003). Analysis of metabolic and physiological responses to gnd knockout in *Escherichia coli* by using C-13 tracer experiment and enzyme activity measurement. *FEMS Microbiology Letters, 220*, 295-301. doi:10.1016/S0378-1097(03)00133-2

Kim, J.H., Wang, C., Jang, H.J., Cha, M.S., Park, J.E., Jo, S.Y., Choi, E.S., & Kim, S.W. (2016). Isoprene production by *Escherichia coli* through the exogenous mevalonate pathway with reduced formation of fermentation byproducts. *Microbial Cell Factories*, *15*, 214. doi: 10.1186/s12934-016-0612-6

Kotlarz, D., Garreau, H., & Buc, H. (1975). Regulation of the amount and of the activity of phosphofructokinases and pyruvate kinases in *Escherichia coli*. *Biochimica et Biophysica Acta, 381,* 257-268.

Kuzuyama, T., & Seto, H. (2012). Two distinct pathways for essential metabolic precursors for isoprenoid biosynthesis. *Proceedings of the Japan Academy, Ser. B, Physical and Biological Sciences, 88*, 41-52. doi:10.2183/pjab.88.41

Lee, S.Y., Choi, J.H., & Xu, Z. (2003). Microbial cell-surface display. *Trends in Biotechnology*, 21, 45-52. doi:10.1016/s0167-7799(02)00006-9

Liu, M., Ding, Y., Chen, H., Zhao, Z., Liu, H., Xian, M., & Zhao, G. (2017). Improving the production of acetyl-CoA-derived chemicals in *Escherichia coli* BL21(DE3)

through iclR and arcA deletion. *BMC Microbiology, 17*, 10. doi: 10.1186/s12866-016-0913-2

Lin, Z., Xu, Z., Li, Y., Wang, Z., Chen, T., Zhao, X. (2014). Metabolic engineering of *Escherichia coli* for the production of riboflavin. *Microbial Cell Factories, 13*, 104. doi: 10.1186/s12934-014-0104-5

Martin, V.J., Pitera, D.J., Withers, S.T., Newman, J.D., & Keasling, J.D. (2003). Engineering a mevalonate pathway in *Escherichia coli* for production of terpenoids. *Nature Biotechnology, 21*, 796-802. doi:10.1038/nbt833

Masuda, A., Toya, Y., & Shimizu, H. (2017). Metabolic impact of nutrient starvation in mevalonate-producing *Escherichia coli*. *Bioresource Technology, 245*, 1634-1640. doi: 10.1016/j.biortech.2017.04.110

Nagai, H., Masuda, A., Toya, Y., Matsuda, F., & Shimizu, H. (2018). Metabolic engineering of mevalonate-producing *Escherichia coli* strains based on thermodynamic analysis. *Metabolic Engineering, 47*, 1-9. doi:

10.1016/j.ymben.2018.02.012

Ohtake, T., Pontrelli, S., Laviña, W.A., Liao, J.C., Putri, S.P., & Fukusaki, E. (2017). Metabolomics-driven approach to solving a CoA imbalance for improved 1-butanol production in *Escherichia coli*. *Metabolic Engineering, 41*, 135-143. doi: 10.1016/j.ymben.2017.04.003

Parimi, N.S., Durie, I.A., Wu, X., Niyas, A.M.M., & Eiteman, M.A. (2017). Eliminating acetate formation improves citramalate production by metabolically engineered *Escherichia coli*. *Microbial Cell Factories, 16*, 114. doi: 10.1186/s12934-017-0729-2

Peng, L., Arauzo-Bravo, M.J., & Shimizu, K. (2004), Metabolic flux analysis for a *ppc* mutant *Escherichia coli* based on 13C-labelling experiments together with enzyme activity assays and intracellular metabolite measurements. *FEMS Microbiology Letters, 235*, 17-23. DOI: 10.1016/j.femsle.2004.04.003

Pitera, D.J., Paddon, C.J., Newman, J.D., & Keasling, J.D. (2007). Balancing a

heterologous mevalonate pathway for improved isoprenoid production in *Escherichia coli*. *Metabolic Engineering, 9*, 193-207. doi: 10.1016/j.ymben.2006.11.002

Rathnasingh, C., Raj, S.M., Lee, Y., Catherine, C., Ashok, S., & Park, S. (2012). Production of 3-hydroxypropionic acid via malonyl-CoA pathway using recombinant *Escherichia coli* strains. *Journal of Biotechnology, 157*, 633-640. doi: 10.1016/j.jbiotec.2011.06.008

Rodriguez, S., Denby, C.M., Van Vu, T., Baidoo, E.E., Wang, G., & Keasling, J.D. (2016). ATP citrate lyase mediated cytosolic acetyl-CoA biosynthesis increases mevalonate production in *Saccharomyces cerevisiae*. *Microbial Cell Factories, 15*, 48. doi: 10.1186/s12934-016-0447-1

Saini, M., Wang, Z.W., Chiang, C.J., & Chao, Y.P. (2014). Metabolic engineering of *Escherichia coli* for production of butyric acid. *Journal of Agricultural and Food Chemistry, 62*, 4342-4348. doi: 10.1021/jf500355p

Siedler, S., Bringer, S., & Bott, M. (2011). Increased NADPH availability in *Escherichia coli*: improvement of the product per glucose ratio in reductive whole-cell biotransformation. *Applied Microbiology and Biotechnology, 92*, 929-937. doi: 10.1007/s00253-011-3374-4

Soma, Y., Inokuma, K., Tanaka, T., Ogino, C., Kondo, A., Okamoto, M., & Hanai, T. (2012). Direct isopropanol production from cellobiose by engineered *Escherichia coli* using a synthetic pathway and a cell surface display system. *Journal of Bioscience and Bioengineering, 114*, 80-85. doi: 10.1016/j.jbiosc.2012.02.019

Soma, Y., Tsuruno, K., Wada, M., Yokota, A., & Hanai, T. (2014). Metabolic flux redirection from a central metabolic pathway toward a synthetic pathway using a metabolic toggle switch. *Metabolic Engineering, 23*, 175-184. doi: 10.1016/j.ymben.2014.02.008

Soma, Y., Yamaji, T., Matsuda, F., & Hanai, T. (2017). Synthetic metabolic bypass for a metabolic toggle switch enhances acetyl-CoA supply for isopropanol

production by *Escherichia coli*. *Journal of Bioscience and Bioengineering,* 123, 625-633. doi: 10.1016/j.jbiosc.2016.12.009

Sukumaran, R.K., Surender, V.J., Sindhu, R., Binod, P., Janu, K.U., Sajna, K.V., Rajasree, K.P., & Pandey, A. (2010). Lignocellulosic ethanol in India: Prospects, challenges and feedstock availability. *Bioresource Technology, 101*, 4826-4833. doi: 10.1016/j.biortech.2009.11.049

Tabata, K., & Hashimoto, S. (2004). Production of mevalonate by a metabolically-engineered *Escherichia coli*. *Biotechnolpgy Letters, 26*, 1487-1491. doi:10.1023/B:BILE.0000044449.08268.7d

Taha, M., Foda, M., Shahsavari, E., Aburto-Medina, A., Adetutu, E., & Ball, A. (2016). Commercial feasibility of lignocellulose biodegradation: possibilities and challenges. *Current Opinion in Biotechnology, 38*, 190-197. doi: 10.1016/j.copbio.2016.02.012

Tamura, G. (2004). Hiochic acid, a new growth factor for *Lactobacillus homohiochi*

and *Lactobacillus heterohiochi*. *Journal of General and Applied Microbiology*, 50, 327-330.

Tanaka, T., Kawabata, H., Ogino, C., & Kondo, A. (2011). Creation of a cellooligosaccharide-assimilating *Escherichia coli* strain by displaying active beta-glucosidase on the cell surface via a novel anchor protein. *Applied and Environmental Microbiology, 77*, 6265-6270. doi: 10.1128/AEM.00459-11

Tanaka, T., Hirata, Y., Nakano, M., Kawabata, H., & Kondo, A. (2014). Creation of cellobiose and xylooligosaccharides-coutilizing *Escherichia coli* displaying both β-glucosidase and β-xylosidase on its cell surface. *ACS Synthetic Biology, 3*, 446-453. doi: 10.1021/sb400070q

Vinopal, R.T., & Fraenkel, D.G. (1975). PfkB and pfkC loci of *Escherichia coli*. *Journal of Bacteriology*, 122, 1153-1161.

Wang, C., Zada, B., Wei, G., & Kim, S.W. (2017). Metabolic engineering and synthetic biology approaches driving isoprenoid production in *Escherichia coli*.

Bioresource Technology, 241, 430-438. doi: 10.1016/j.biortech.2017.05.168

Wang, J., Niyompanich, S., Tai, Y.S., Wang, J., Bai, W., Mahida, P., Gao, T., & Zhang, K. (2016). Engineering of a Highly Efficient *Escherichia coli* Strain for Mevalonate Fermentation through Chromosomal Integration. *Applied and Environmental Microbiology, 82*, 7176-7184. doi:10.1128/AEM.02178-16

Wang, Q., Xu, J., Sun, Z., Luan, Y., Li, Y., Wang, J., Liang, Q., & Qi, Q. (2018). Engineering an in vivo EP-bifido pathway in *Escherichia coli* for high-yield acetyl-CoA generation with low CO_2 emission. *Metabolic Engineering*, 51, 79-87 doi: 10.1016/j.ymben.2018.08.003

Wang, Y., San, K.Y., & Bennett, G.N. (2013). Improvement of NADPH bioavailability in *Escherichia coli* by replacing NAD(+)-dependent glyceraldehyde-3-phosphate dehydrogenase GapA with NADP (+)-dependent GapB from *Bacillus subtilis* and addition of NAD kinase. *Journal of Industrial Microbiology and Biotechnology, 40*, 1449-1460. doi: 10.1007/s10295-013-1335-x

Ward, V.C.A., Chatzivasileiou, A.O., & Stephanopoulos, G. (2018). Metabolic engineering of *Escherichia coli* for the production of isoprenoids. *FEMS Microbiology Letters, 365*, fny079. doi: 10.1093/femsle/fny079

Wu, X., & Eiteman, M.A. (2016). Production of citramalate by metabolically engineered *Escherichia coli*. *Biotechnology and Bioengineering, 113*, 2670-2675. doi: 10.1002/bit.26035

Xiong, M., Schneiderman, D.K., Bates, F.S., Hillmyer, M.A., & Zhang, K. (2014). Scalable production of mechanically tunable block polymers from sugar. P*roceedings of the National Academy of Sciences of the United States of America*, *111,* 8357-8362. doi: 10.1073/pnas.1404596111

Xu, D., & Zhang, L. (2019) Increasing Agmatine Production in *Escherichia coli* through Metabolic Engineering. *Journal of Agricultural and Food Chemistry*, 67, 7908-7915. doi: 10.1021/acs.jafc.9b03038

Zheng, Y., Yuan, Q., Yang, X., Ma, H. (2017). Engineering *Escherichia coli* for poly-

(3-hydroxybutyrate) production guided by genome-scale metabolic network analysis. *Enzyme and Microbial Technology, 106*, 60-66. doi:10.1016/j.enzmictec.2017.07.003

Figure captions

Figure 1. Metabolic pathway for producing mevalonate and the characteristics of plasmids used in this study. (a) Metabolic design for improving mevalonate production. (b) Plasmids used in this study. (c) Mevalonate production using the *E. coli* MG1655 strain harboring each plasmid after 48 h of cultivation. The experiments were performed in triplicate and error bars indicate the standard deviation.

Figure 2. Mevalonate production using gene-deficient *E. coli* strains for improvements of NADPH regeneration. The ratio of NADPH/$NADP^+$ (a), mevalonate titers (b), and cellular growth (c) after 48 h of cultivation using 20 g/L of glucose as a carbon source are shown. The experiments were performed in triplicate and error bars indicate standard deviation.

Figure 3. Mevalonate production using gene-deficient *E. coli* strains to improve the supply of acetyl-CoA. The amount of intracellular acetyl-CoA (a), mevalonate titers (b), and cellular growth rates (c) after 48 h of cultivation using 20 g/L of glucose as a

carbon source are shown. The experiments were performed in triplicate and error bars indicate standard deviation.

Figure 4. Culture profiles of mevalonate-producing strains using glucose as a carbon source. Mevalonate production (a), cellular growth (b), and glucose consumption (c) are shown. Cells were cultivated in M9Y medium containing 20 g/L glucose. The experiments were performed in triplicate and error bars indicate standard deviation.

Figure 5. Mevalonate production using gene-deficient *E. coli* strains using 20 g/L cellobiose as a carbon source. Mevalonate titers (a) and cellular growth (b) after 48 h of cultivation. The experiments were performed in triplicate and error bars indicate standard deviation.

Figure 6. Culture profiles of mevalonate-producing strains using cellobiose as a carbon source. Mevalonate production (a), cellular growth (b), cellobiose (c), and glucose consumption (d), the amount of intracellular acetyl-CoA after 8h cultivation (e),

mevalonate titers after 8h cultivation (f) are shown. Cells were cultivated in the M9Y medium containing 20 g/L cellobiose. The experiments were performed in triplicate and error bars indicate standard deviation.

a

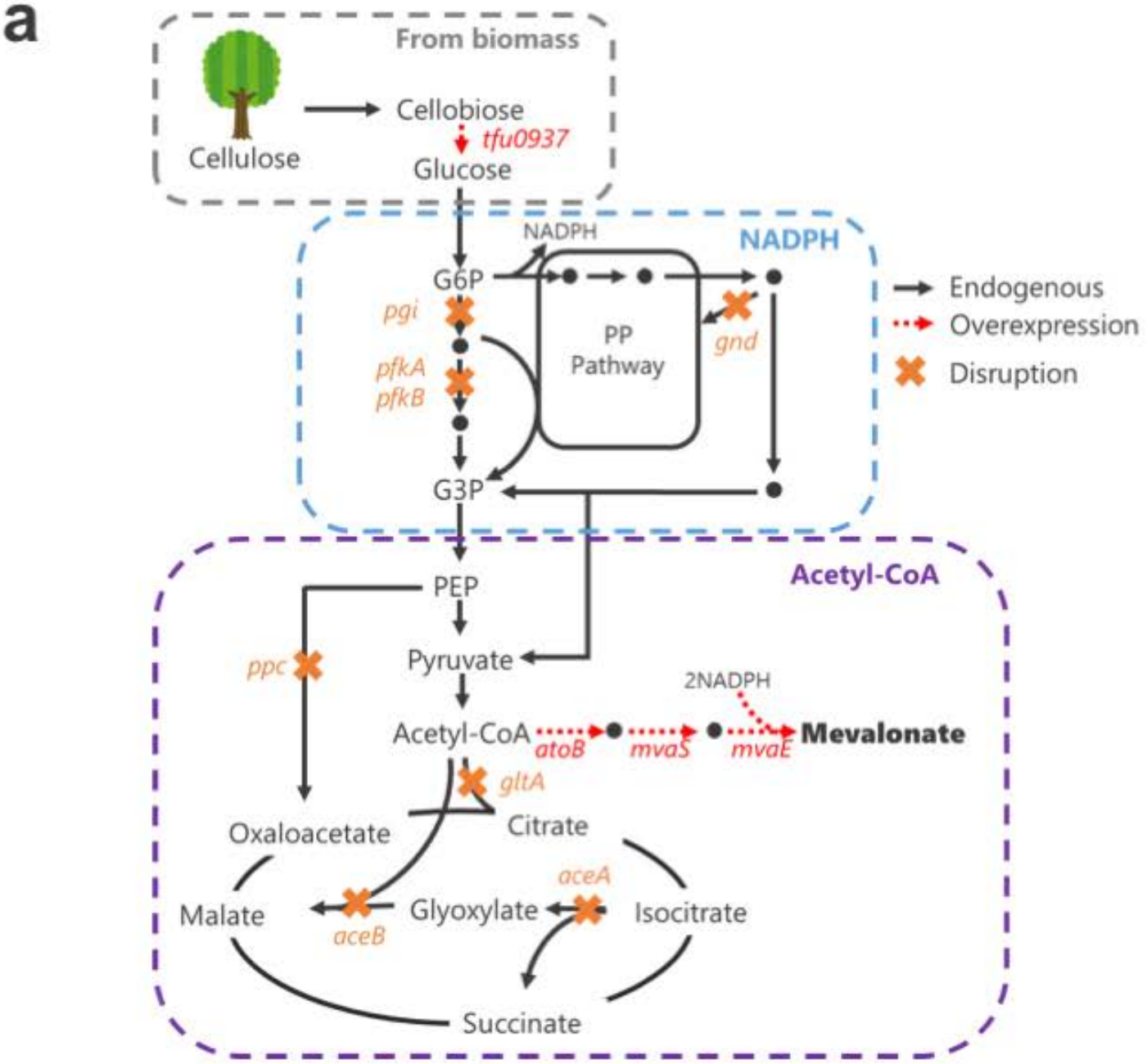
From biomass
Cellulose
Cellobiose
tfu0937
Glucose
NADPH
NADPH
G6P
pgi
pfkA
pfkB
PP
Pathway
gnd
G3P
Endogenous
Overexpression
Disruption
Acetyl-CoA
PEP
ppc
Pyruvate
2NADPH
Acetyl-CoA
atoB
mvaS
mvaE
Mevalonate
gltA
Oxaloacetate
Citrate
aceA
Malate
aceB
Glyoxylate
Isocitrate
Succinate

b

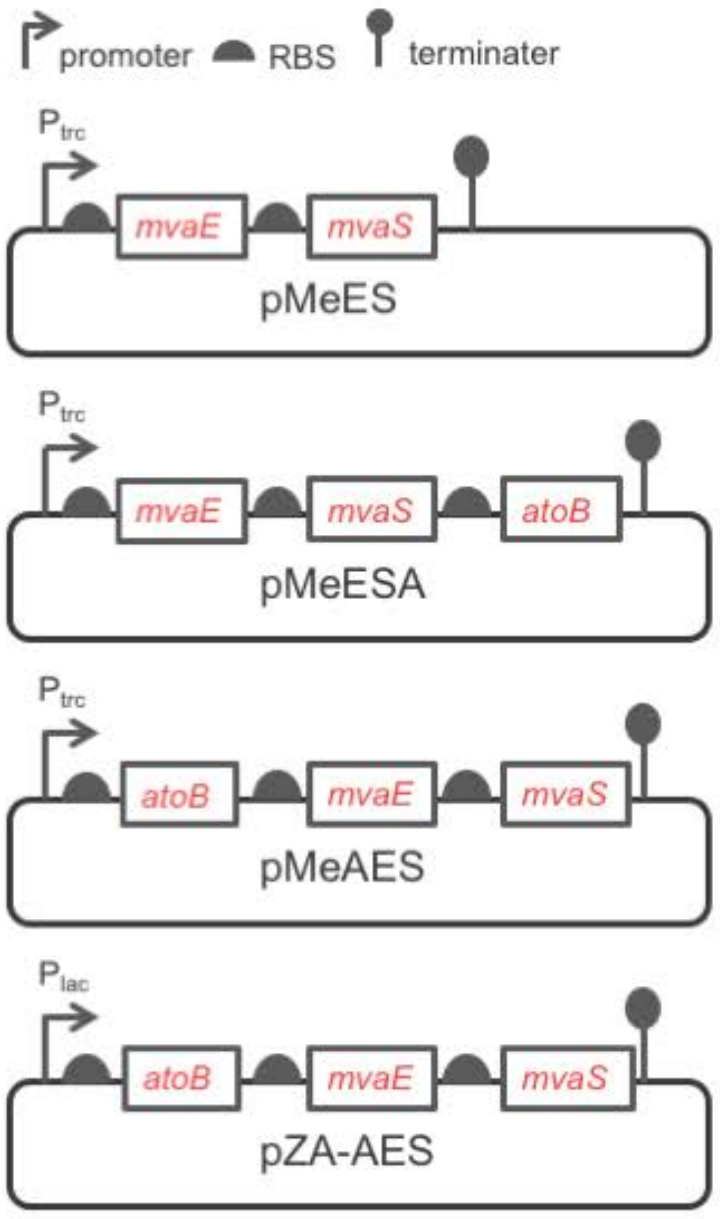
promoter
RBS
terminater
Ptrc
mvaE
mvaS
pMeES
Ptrc
mvaE
mvaS
atoB
pMeESA
Ptrc
atoB
mvaE
mvaS
pMeAES
Plac
atoB
mvaE
mvaS
pZA-AES

c

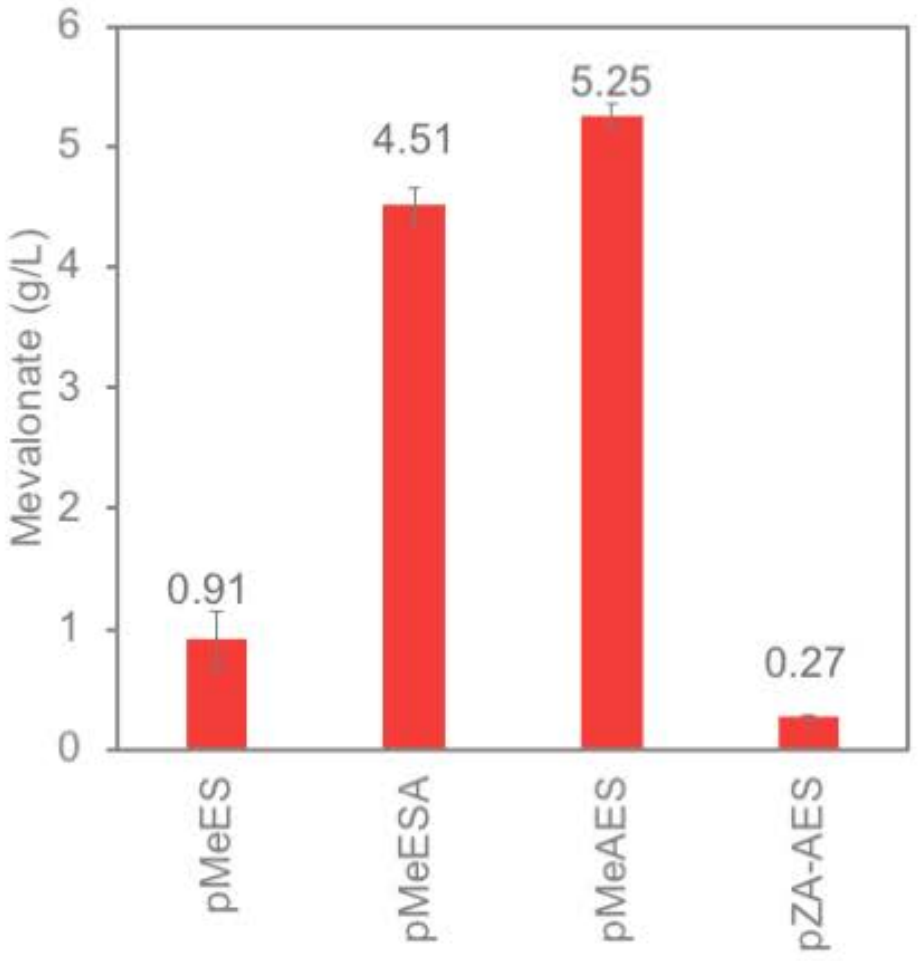
Mevalonate (g/L)
0
1
2
3
4
5
6
0.91
4.51
5.25
0.27
pMeES
pMeESA
pMeAES
pZA-AES

a

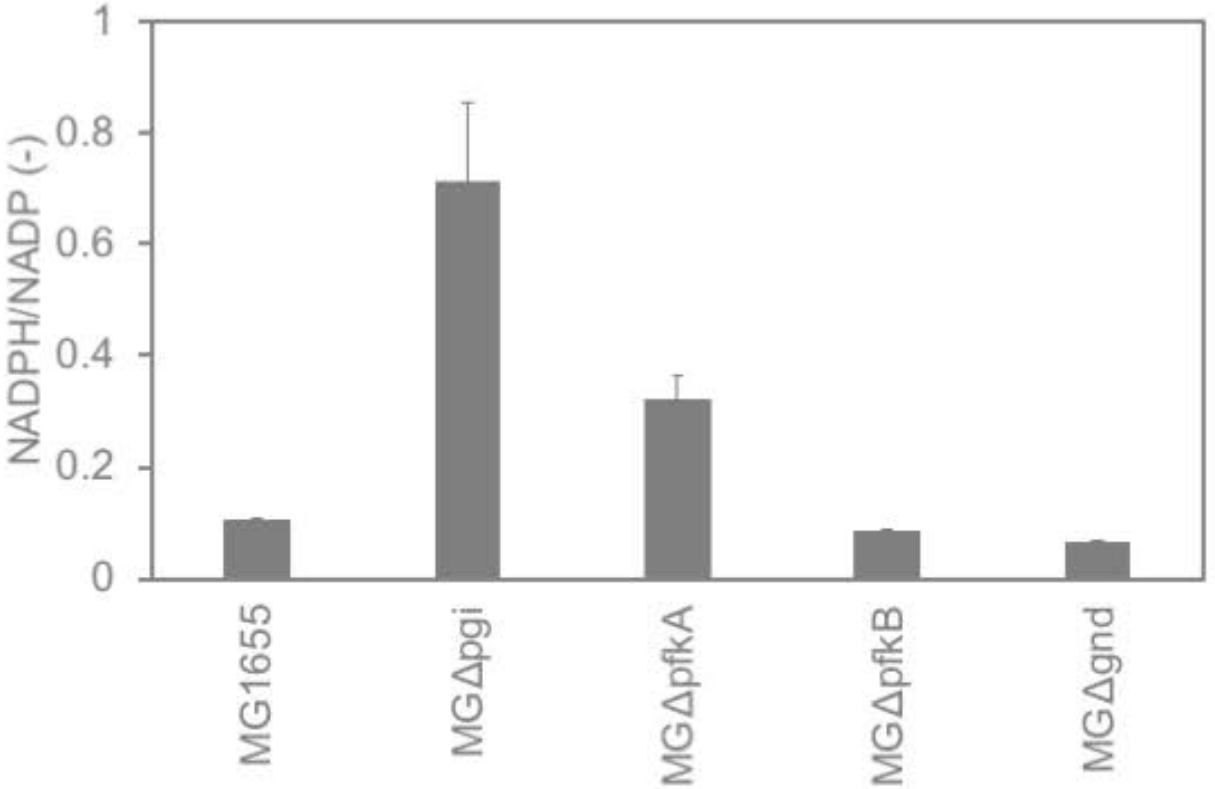
NADPH/NADP (-)
1
0.8
0.6
0.4
0.2
0
MG1655
MGΔpgi
MGΔpfkA
MGΔpfkB
MGΔgnd

b

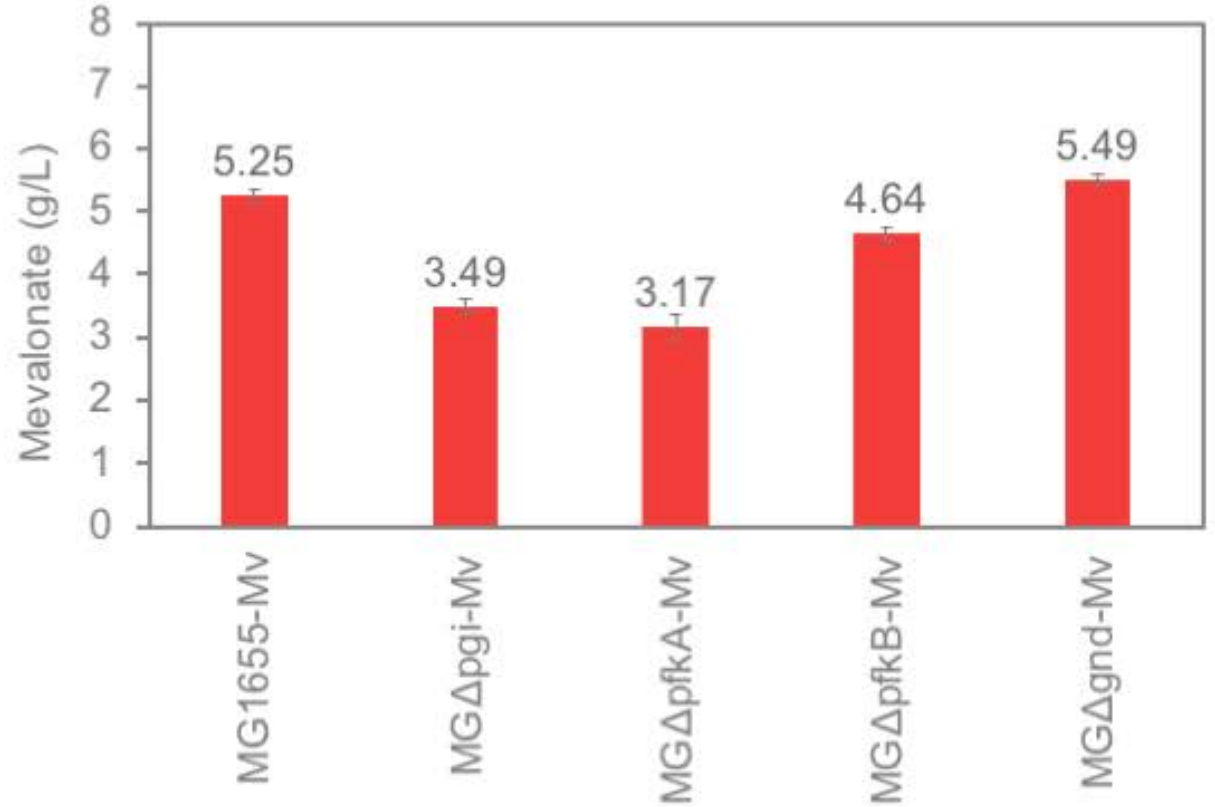
Mevalonate (g/L)
8
7
6
5
4
3
2
1
0
5.25
3.49
3.17
4.64
5.49
MG1655-Mv
MGΔpgi-Mv
MGΔpfkA-Mv
MGΔpfkB-Mv
MGΔgnd-Mv

c

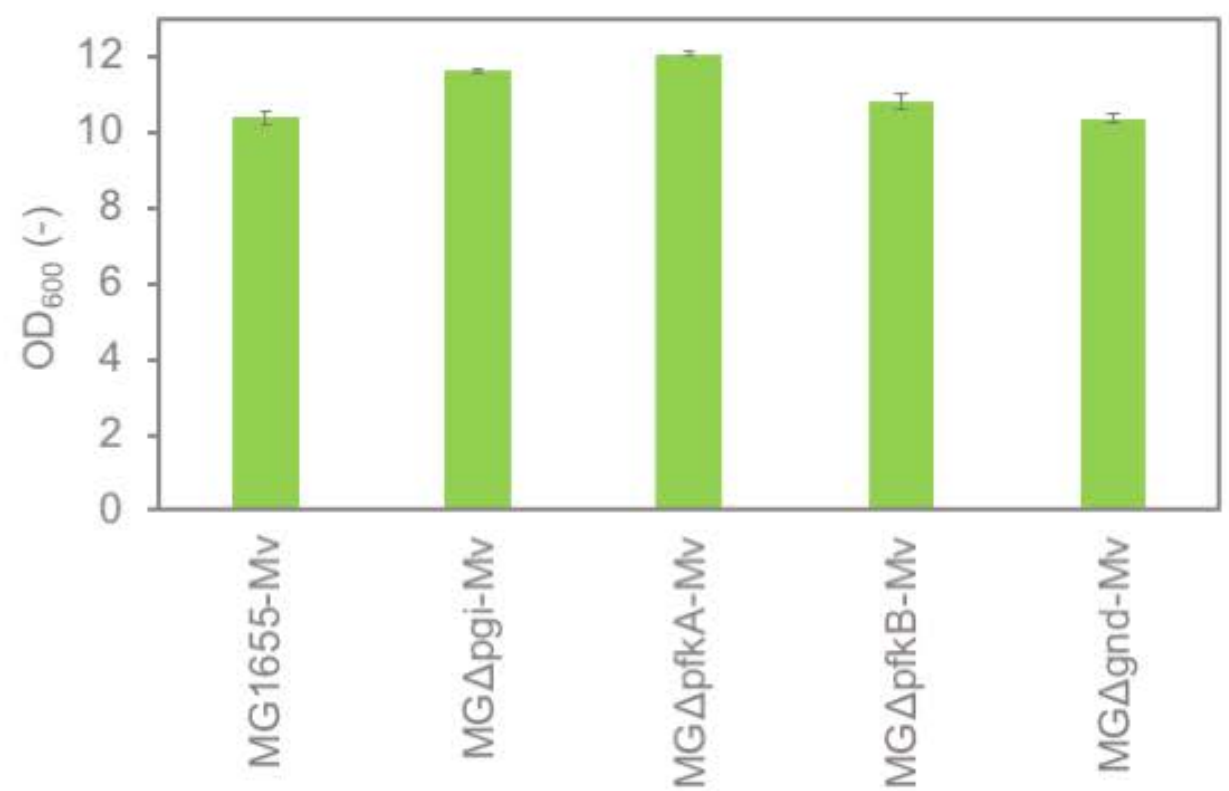
OD600 (-)
12
10
8
6
4
2
0
MG1655-Mv
MGΔpgi-Mv
MGΔpfkA-Mv
MGΔpfkB-Mv
MGΔgnd-Mv

a

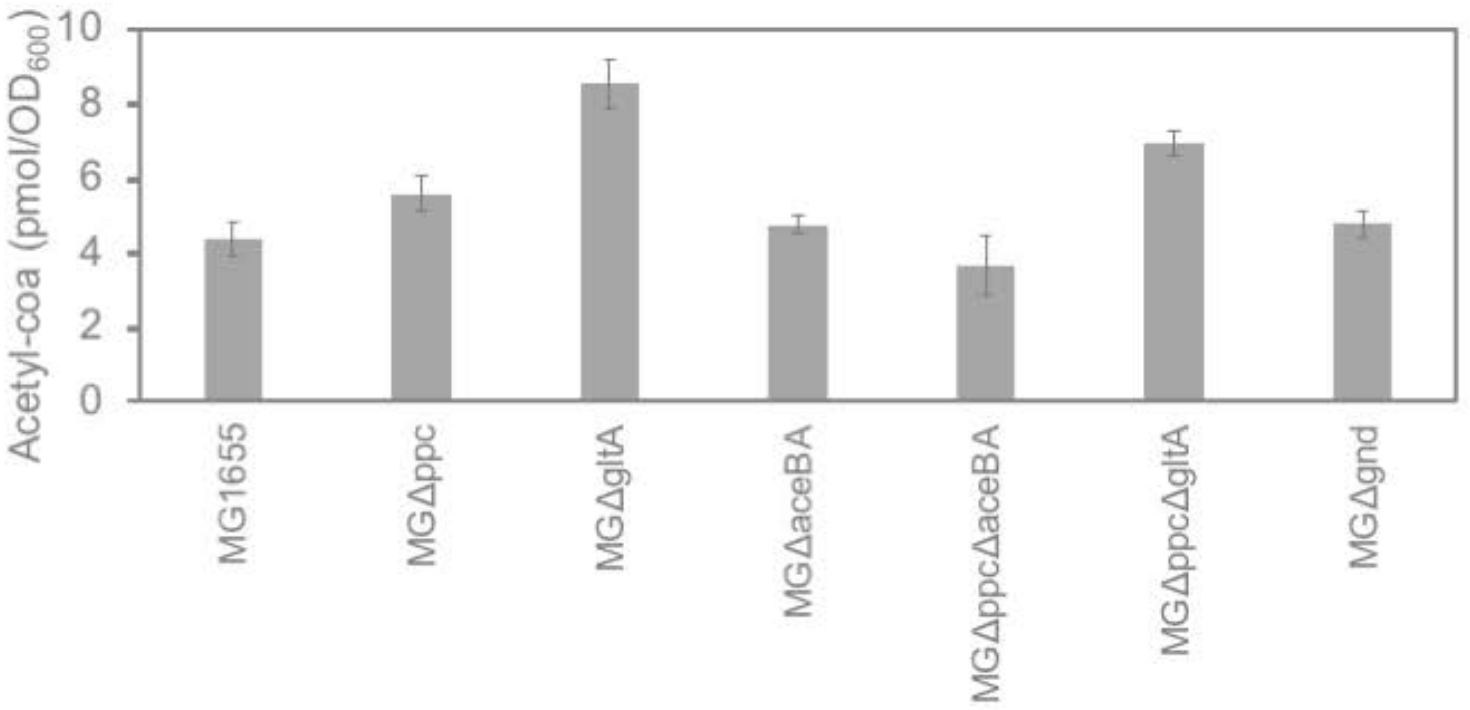
Acetyl-coa (pmol/OD600)
0
2
4
6
8
10
MG1655
MGΔppc
MGΔgltA
MGΔaceBA
MGΔppcΔaceBA
MGΔppcΔgltA
MGΔgnd

b

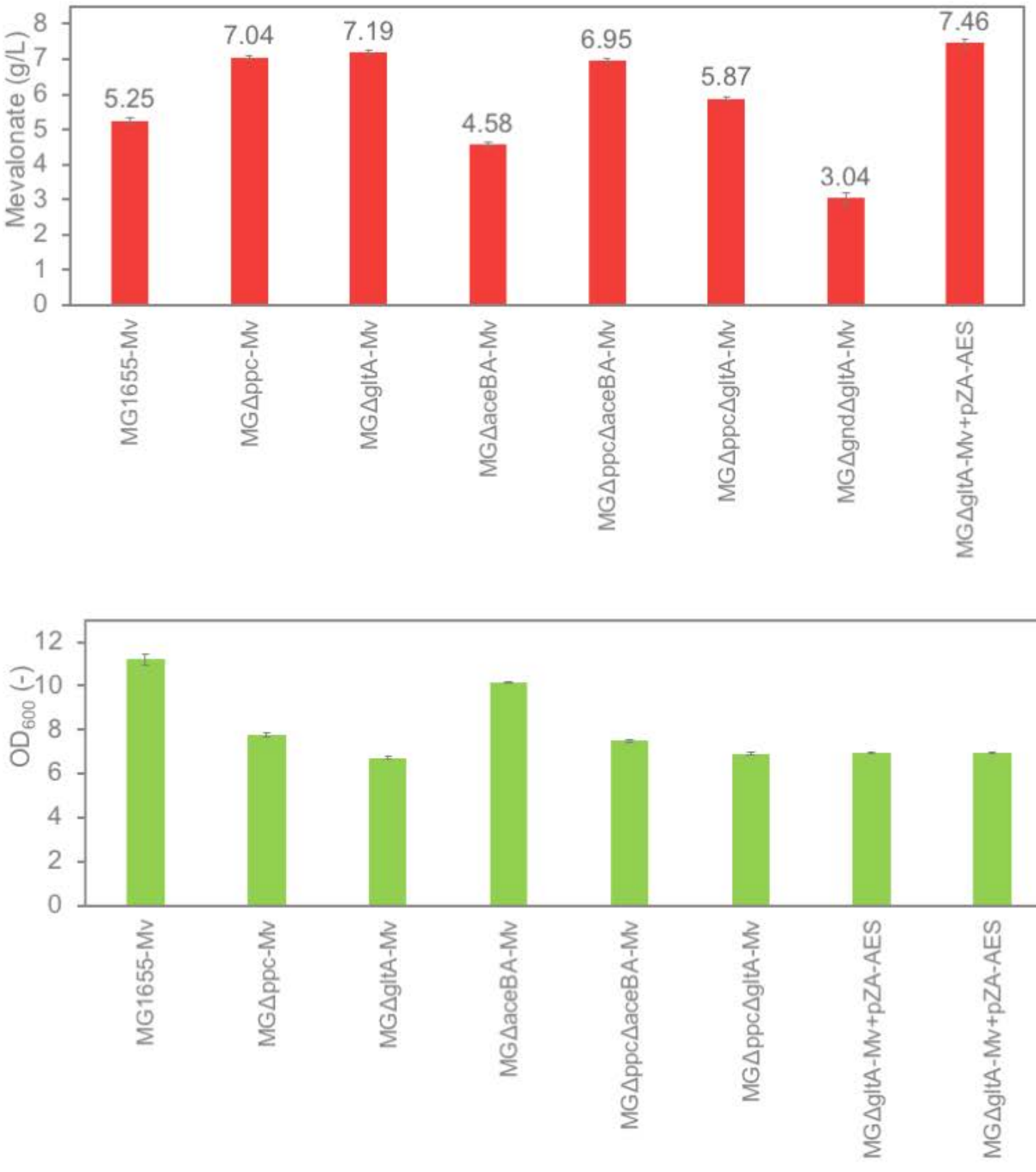
Mevalonate (g/L)
0
1
2
3
4
5
6
7
8
5.25
7.04
7.19
4.58
6.95
5.87
3.04
7.46
MG1655-Mv
MGΔppc-Mv
MGΔgltA-Mv
MGΔaceBA-Mv
MGΔppcΔaceBA-Mv
MGΔppcΔgltA-Mv
MGΔgndΔgltA-Mv
MGΔgltA-Mv+pZA-AES

c

OD600 (-)
0
2
4
6
8
10
12
MG1655-Mv
MGΔppc-Mv
MGΔgltA-Mv
MGΔaceBA-Mv
MGΔppcΔaceBA-Mv
MGΔppcΔgltA-Mv
MGΔgltA-Mv+pZA-AES
MGΔgltA-Mv+pZA-AES

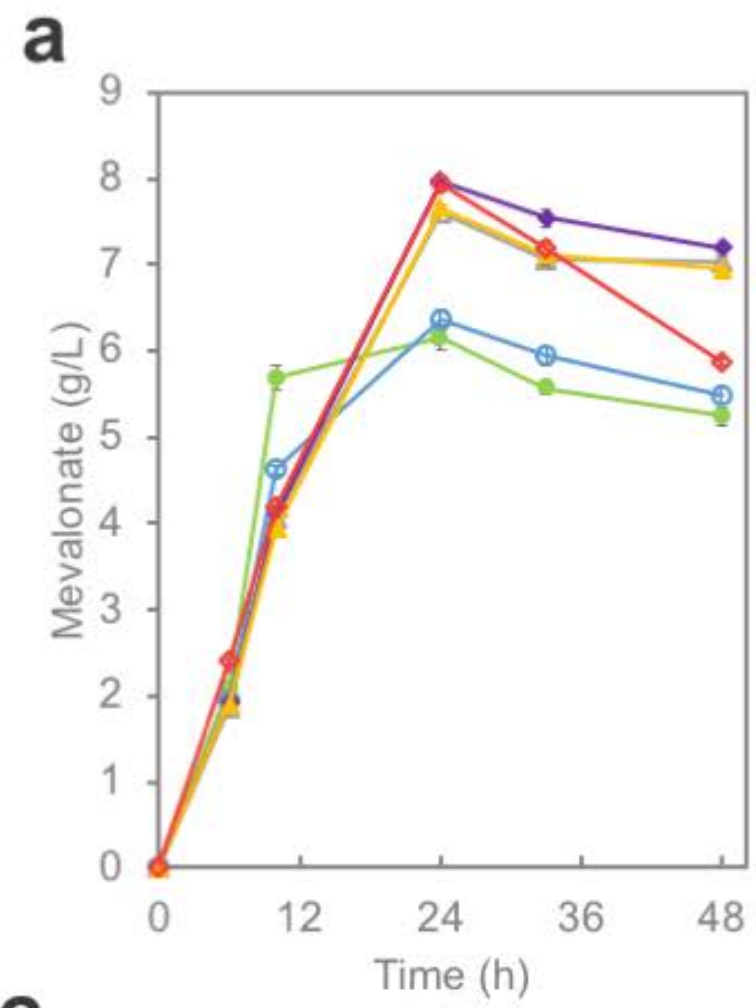
a
Mevalonate (g/L)
0
1
2
3
4
5
6
7
8
9
0
12
24
36
48
Time (h)

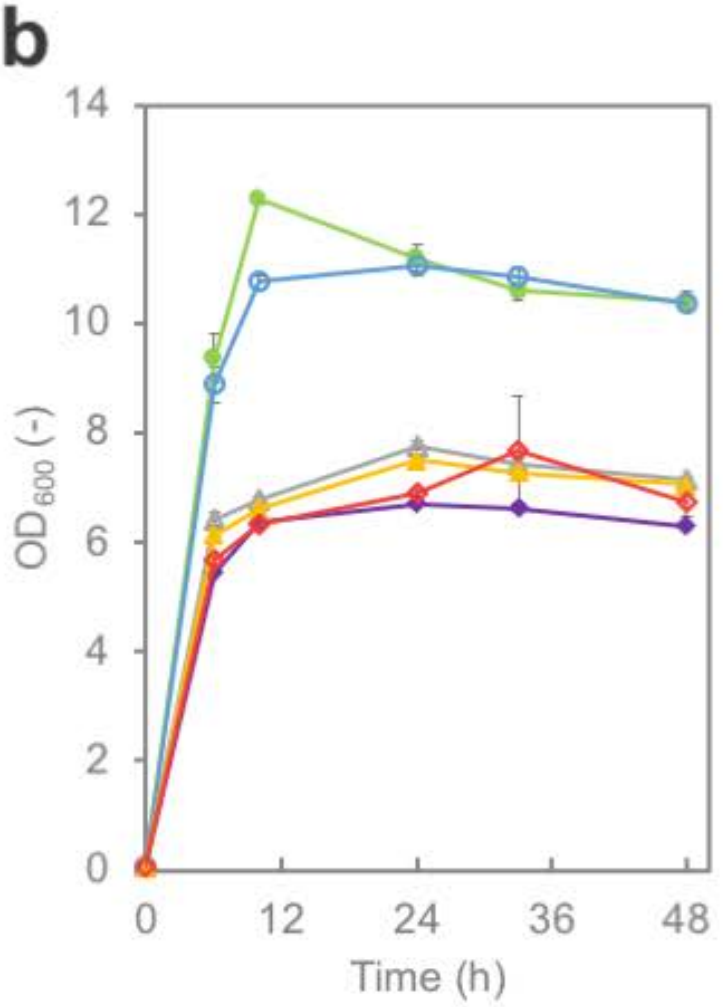
b
OD600 (-)
0
2
4
6
8
10
12
14
0
12
24
36
48
Time (h)

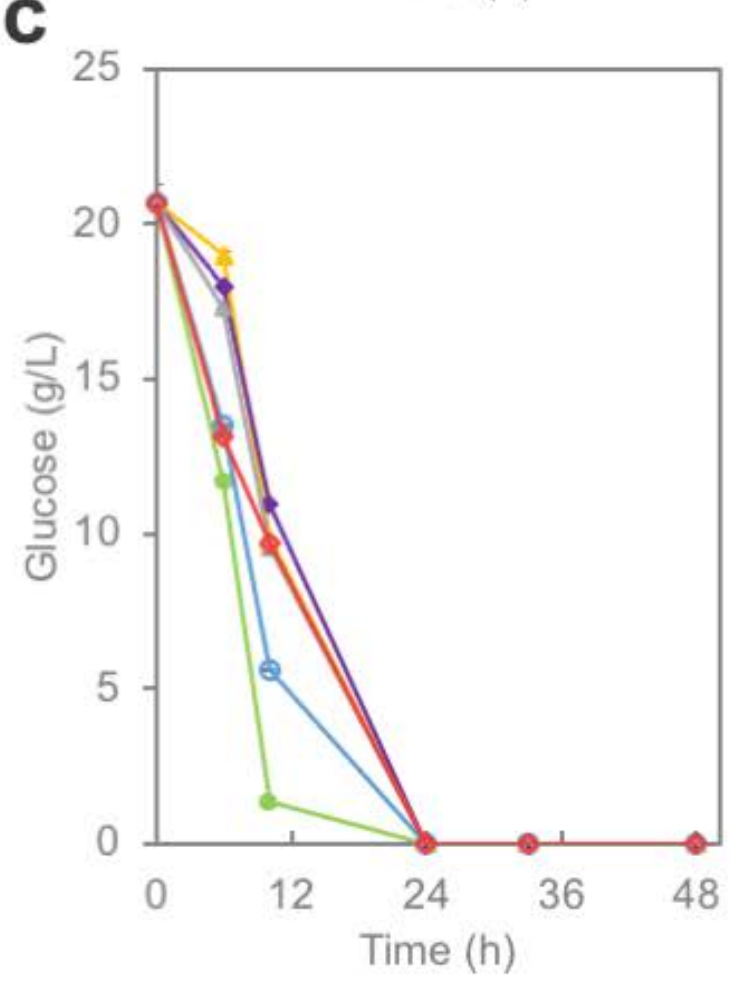
c
Glucose (g/L)
0
5
10
15
20
25
0
12
24
36
48
Time (h)

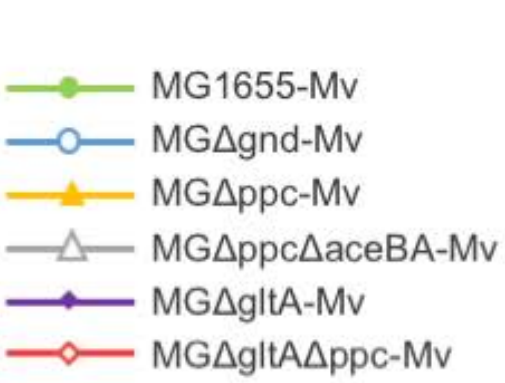
MG1655-Mv
MGΔgnd-Mv
MGΔppc-Mv
MGΔppcΔaceBA-Mv
MGΔgltA-Mv
MGΔgltAΔppc-Mv

a

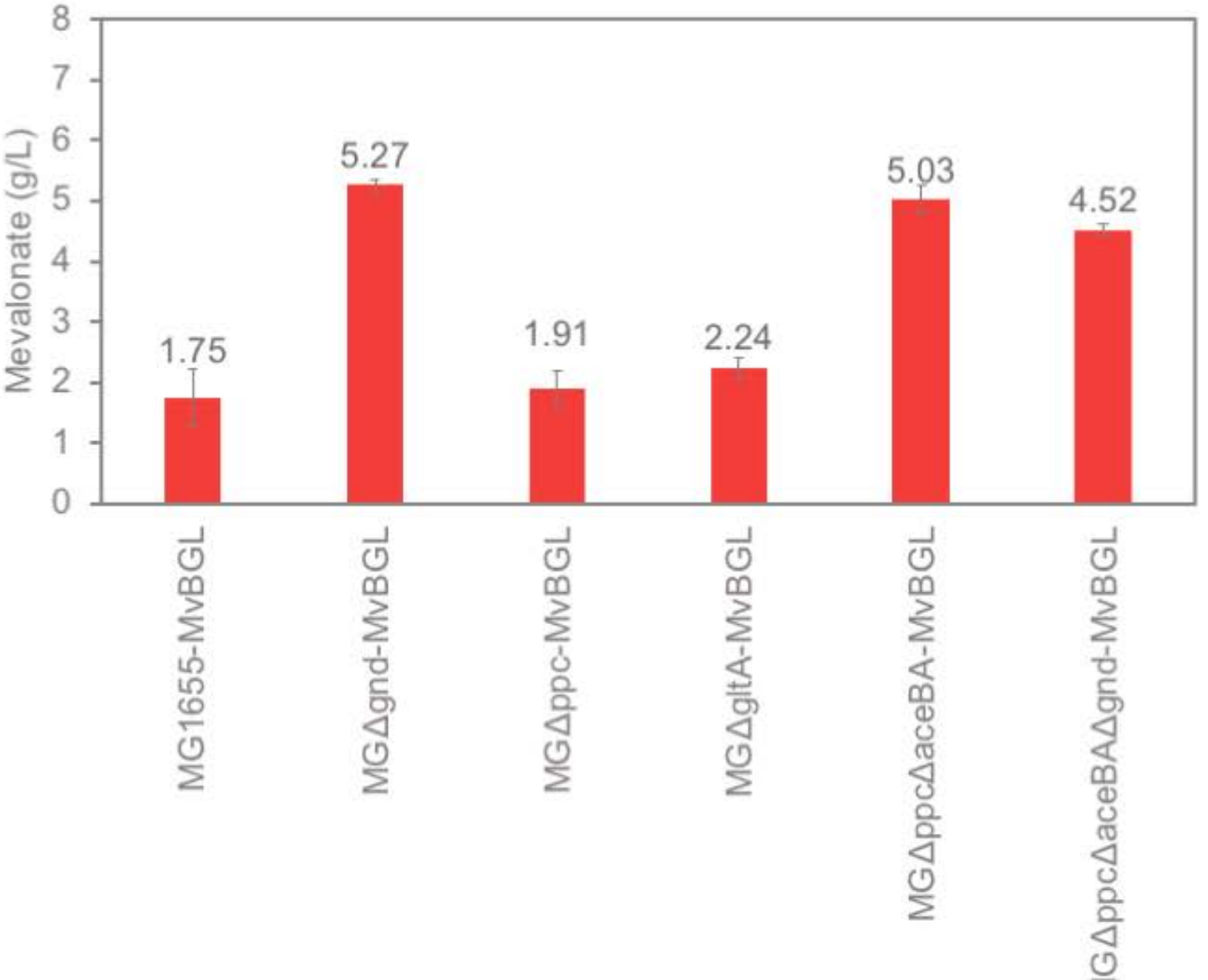
Mevalonate (g/L)
0
1
2
3
4
5
6
7
8
1.75
5.27
1.91
2.24
5.03
4.52
MG1655-MvBGL
MGΔgnd-MvBGL
MGΔppc-MvBGL
MGΔgltA-MvBGL
MGΔppcΔaceBA-MvBGL
MGΔppcΔaceBAΔgnd-MvBGL

b

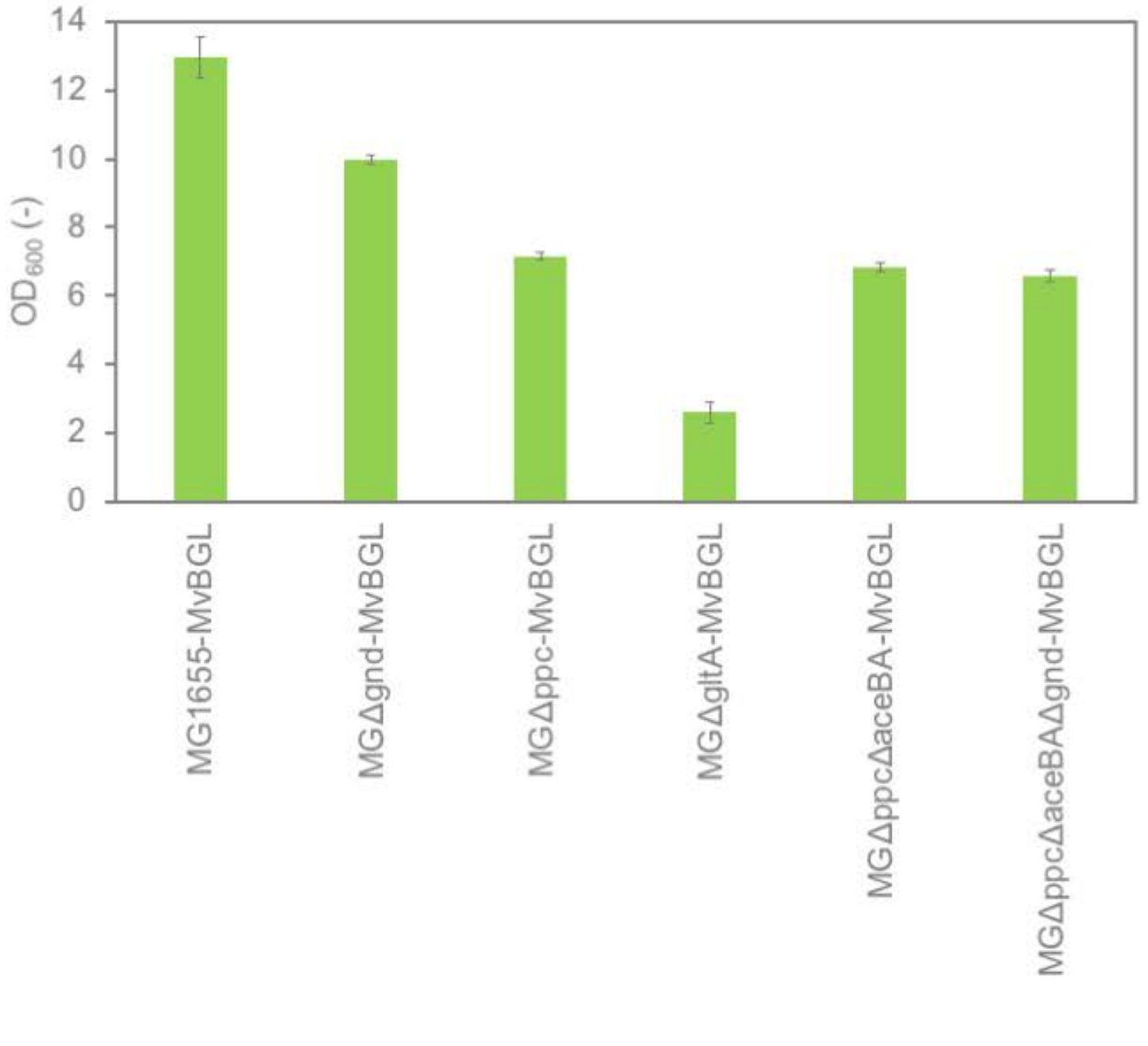
OD600 (-)
0
2
4
6
8
10
12
14
MG1655-MvBGL
MGΔgnd-MvBGL
MGΔppc-MvBGL
MGΔgltA-MvBGL
MGΔppcΔaceBA-MvBGL
MGΔppcΔaceBAΔgnd-MvBGL

a

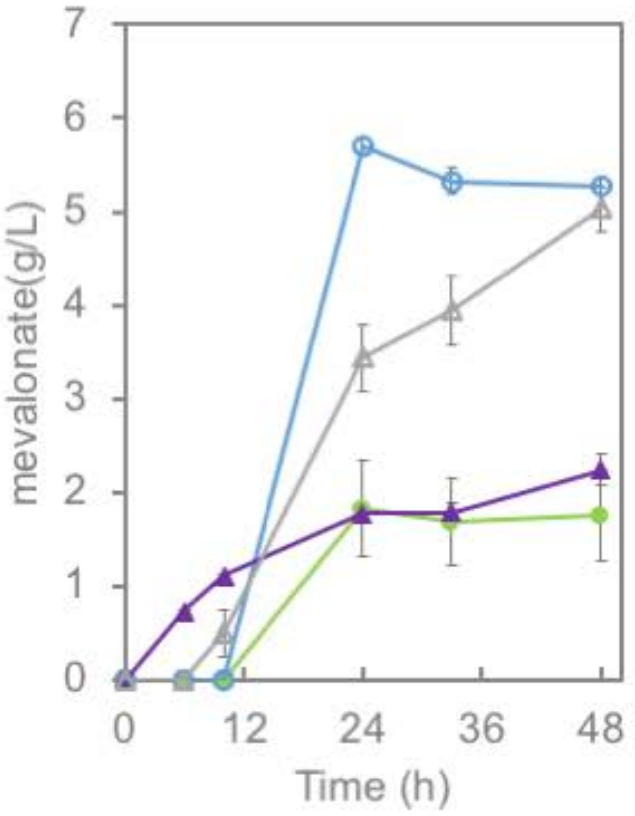
mevalonate(g/L)
0
1
2
3
4
5
6
7
0
12
24
36
48
Time (h)

b

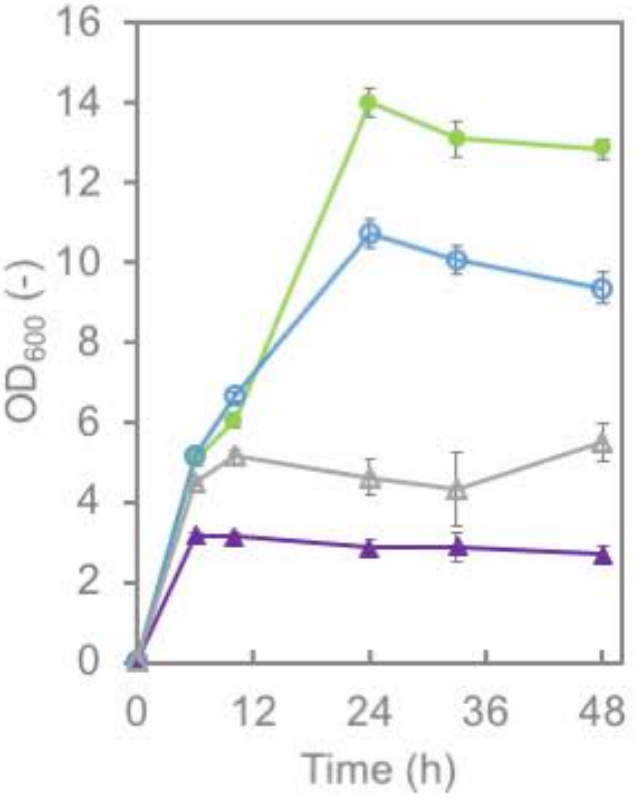
OD600 (-)
0
2
4
6
8
10
12
14
16
0
12
24
36
48
Time (h)

c

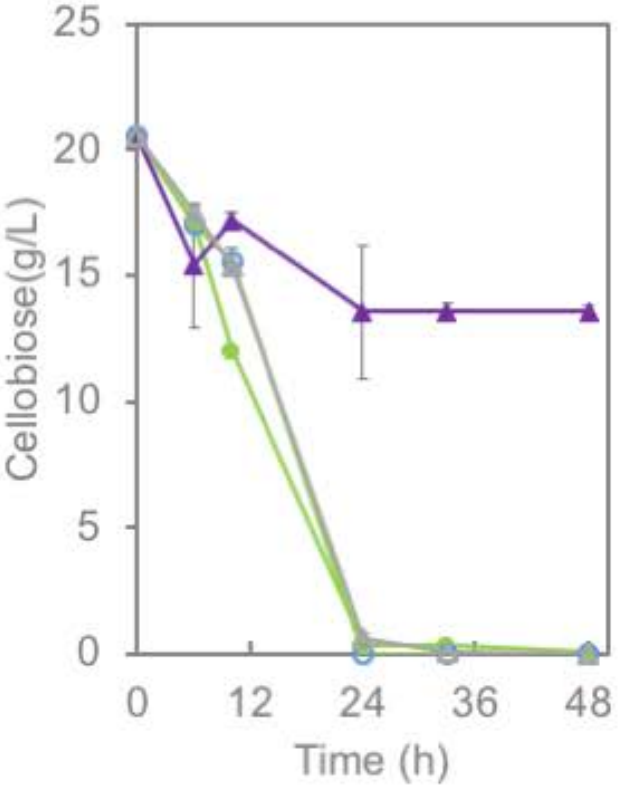
Cellobiose(g/L)
0
5
10
15
20
25
0
12
24
36
48
Time (h)

d

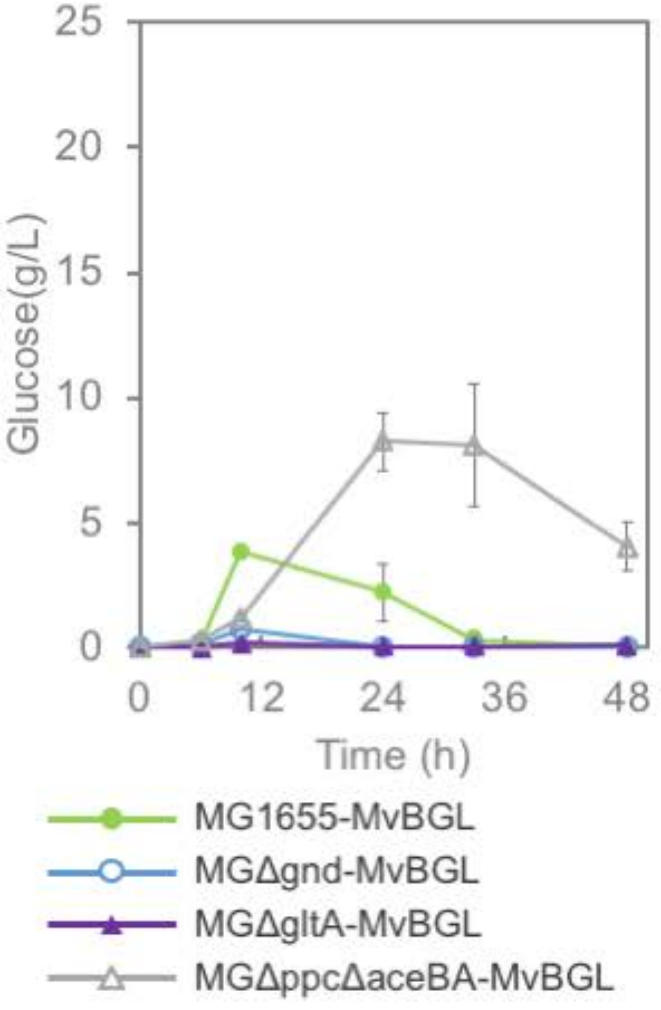
Glucose(g/L)
0
5
10
15
20
25
0
12
24
36
48
Time (h)
MG1655-MvBGL
MGΔgnd-MvBGL
MGΔgltA-MvBGL
MGΔppcΔaceBA-MvBGL

e

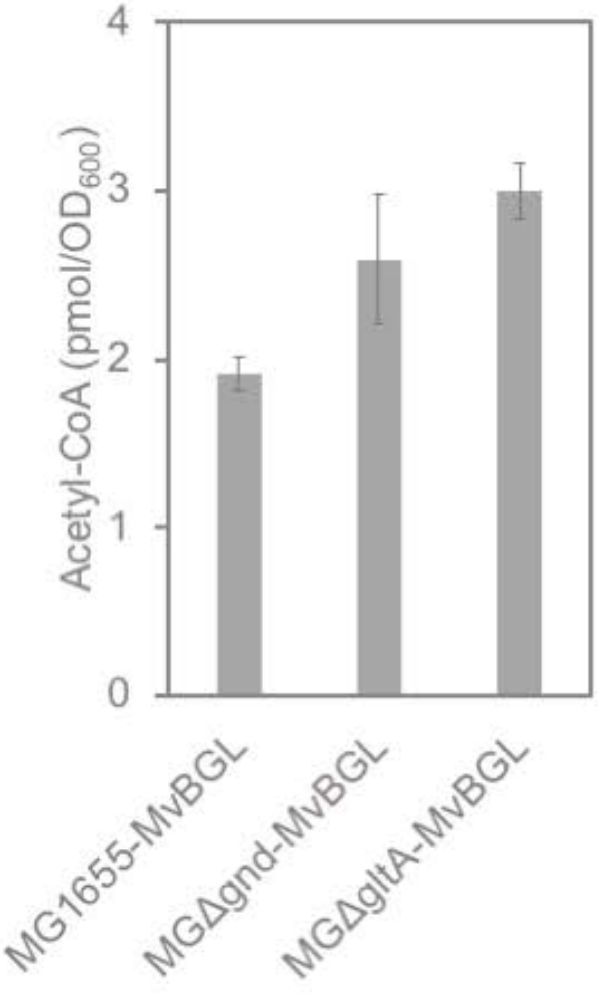
Acetyl-CoA (pmol/OD600)
0
1
2
3
4
MG1655-MvBGL
MGΔgnd-MvBGL
MGΔgltA-MvBGL

f

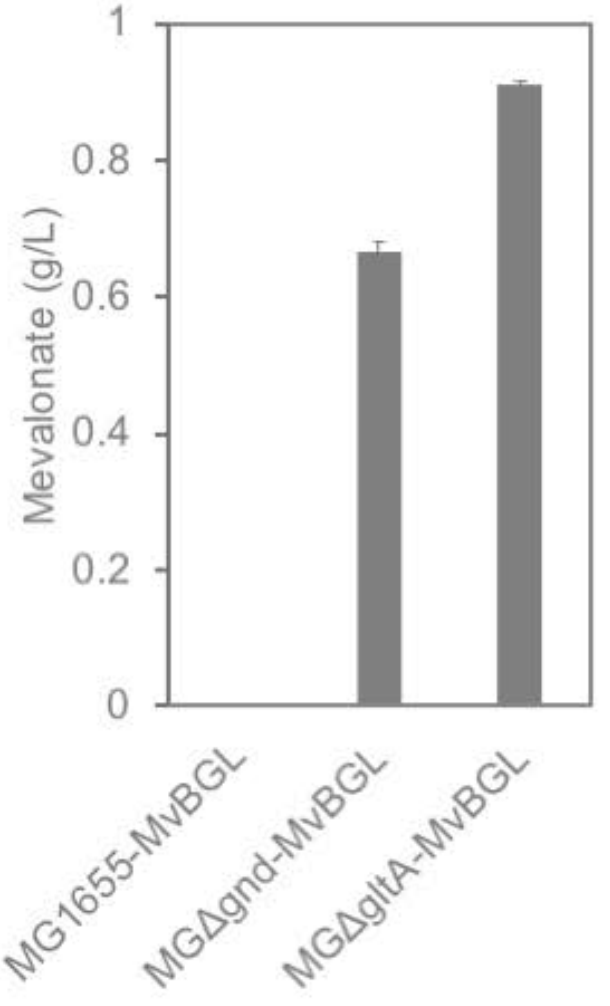
Mevalonate (g/L)
0
0.2
0.4
0.6
0.8
1
MG1655-MvBGL
MGΔgnd-MvBGL
MGΔgltA-MvBGL

Table

Table 1. Strains and Plasmids

Strains		
Nova Blue	*endA1, hsdR17,*($r_K^-m_K^+$), *supE44 thi-I*, gyrA96, *relA1*, *lac*, *recA1*/F′, [*proAB*$^+$, *lacI*q ZΔM15,Tn10(Tet ^{R})]	Novagen
MG1655	*Escherichia coli* K-12 MG1655	Bachmann 1972
MGΔpgi	MG1655Δ*pgi*	This study
MGΔpfkA	MG1655Δ*pfkA*	This study
MGΔpfkB	MG1655Δ*pfkB*	This study
MGΔgnd	MG1655Δ*gnd*	This study
MGΔaceBA	MG1655Δ*aceBA*	This study
MGΔppc	MG1655Δ*ppc*	This study
MGΔppcΔaceBA	MG1655Δ*ppc*Δ*aceBA*	This study
MGΔppcΔaceBAΔgnd	MG1655Δ*ppc*Δ*aceBA*Δ*gnd*	This study
MGΔgltA	MG1665Δ*gltA*	This study
MGΔppcΔgltA	MG1655Δ*ppc*Δ*gltA*	This study
MGΔgltAΔgnd	MG1655Δ*gltA*Δ*gnd*	This study
MG1655-Mv	MG1655 harboring pMeAES	This study
MGΔpgi-Mv	MG1655Δ*pgi* harboring pMeAES	This study
MGΔpfkA-Mv	MG1655Δ*pfkA* harboring pMeAES	This study
MGΔpfkB-Mv	MG1655Δ*pfkB* harboring pMeAES	This study
MGΔgnd-Mv	MG1655Δ*gnd* harboring pMeAES	This study

MGΔaceBA-Mv	MG1655Δ*aceBA* harboring pMeAES	This study
MGΔppc-Mv	MG1655Δ*ppc* harboring pMeAES	This study
MGΔppcΔaceBA-Mv	MG1655Δ*ppc*Δ*aceBA* harboring pMeAES	This study
MGΔppcΔaceBAΔgnd-Mv	MG1655Δ*ppc*Δ*aceBA*Δ*gnd* harboring pMeAES	This study
MGΔgltA-Mv	MG1665Δ*gltA* harboring pMeAES	This study
MGΔppcΔgltA-Mv	MG1655Δ*ppc*Δ*gltA* harboring pMeAES	This study
MGΔgltAΔgnd-Mv	MG1655Δ*gltA*Δ*gnd* harboring pMeAES	This study
MGΔgltA-Mv+pZA-AES	MG1665Δ*gltA* harboring pMeAES and pZA-AES	This study
MG1655-MvBGL	MG1655 harboring pMeAES-BGL	This study
MGΔpfkB-MvBGL	MG1655Δ*pfkB* harboring pMeAES-BGL	This study
MGΔgnd-MvBGL	MG1655Δ*gnd* harboring pMeAES-BGL	This study
MGΔppc-MvBGL	MG1655Δ*ppc* harboring pMeAES-BGL	This study
MGΔppcΔaceBA-MvBGL	MG1655Δ*ppc*Δ*aceBA* harboring pMeAES-BGL	This study
MGΔppcΔaceBAΔgnd-MvBGL	MG1655Δ*ppc*Δ*aceBA*Δ*gnd* harboring pMeAES-BGL	This study
MGΔgltA-MvBGL	MG1665Δ*gltA* harboring pMeAES-BGL	This study

Plasmids

pTrcHisB	P_{trc}, pBR322 ori and Amp^r	Life Technologies
pZA23	$P_{A1lacO-1}$, p15A ori and Kn^r	Expressys
pMeES	pTrcHisB-*mvaE-mvaS*	This study
pMeESA	pTrcHisB-*mvaE-mvaS-atoB*	This study
pMeAES	pTrcHisB-*atoB-mvaE-mvaS*	This study

pZA-ASE	pZA23-*atoB-mvaE-mvaS*	This study
pZA-XPK	pZA23-*fxpk-fbp*	This study
pHLA-BGL	Vector for Tfu0937 expression using Blc anchor protein; the C terminus of Blc was fused to the N terminus of Tfu0937	Tanaka et al. 2011
pMeAES-BGL	pTrcHisB-*atoB-mvaE-mvaS*-P_{HCE}-*blc-tfu0937*	This study
pTargetF	Constitutive expression of sgRNA	Addgene
pCas	Constitutive expression of cas9 and inducible expression of λ RED and sgRNA	Addgene
pTΔpgi	Constitutive expression of sgRNA wirh donor editing template DNA for *pgi* disruption	This study
pTΔpfkA	Constitutive expression of sgRNA wirh donor editing template DNA for *pfkA* disruption	This study
pTΔpfkB	Constitutive expression of sgRNA wirh donor editing template DNA for *pfkB* disruption	This study
pTΔgnd	Constitutive expression of sgRNA wirh donor editing template DNA for *gnd* disruption	This study
pTΔaceBA	Constitutive expression of sgRNA wirh donor editing template DNA for *aceBA* disruption	This study
pTΔppc	Constitutive expression of sgRNA wirh donor editing template DNA for *ppc* disruption	This study
pTΔgltA	Constitutive expression of sgRNA wirh donor editing template DNA for *gltA* disruption	This study

Supporting Information

Metabolic engineering of *E. coli* for improving mevalonate production to promote NADPH regeneration and enhance acetyl-CoA supply

Satowa et al.,

1. Strains and plasmid construction

The strains and plasmids used in this study are listed in Table 1. E. coli NovaBlue competent cells (Novagen, Cambridge, MA, USA) were used for gene cloning. Polymerase chain reaction (PCR) was performed using KOD FX (TOYOBO, Osaka, Japan). Custom DNA oligonucleotide primers were obtained from Invitrogen Custom DNA Oligos (Thermo Fisher Scientific, Tokyo, Japan). Codon-optimized genes fragments (mvaS and mvaE, both from E. faecalis) were provided by the Invitrogen GeneArt Gene Synthesis service (Thermo Fisher Scientific, Tokyo, Japan). The sequences of primers and genes fragments are shown in Table S1 and Table S2, respectively.

Plasmids for mevalonate production were constructed as follows. The linearized fragment was amplified by inverse PCR using pTrcHisB (Thermo Fisher Scientific) as a template with the Inv_pTrcB_Fw and Inv_pTrcB_Rv primers. This linearized fragment was ligated using Gibson Assembly (New England BioLabs Japan, Tokyo, Japan) using the synthetic gene mvaE. The resulting plasmid was designated pTrcHisB-mvaE. The synthetic gene mvaS was cloned into the KpnI site of pTrcHisB-mvaE, and the resulting plasmid was designated pMeES. The linearized fragment was amplified by inverse PCR using pMeES as a template with the primer pair Inv_pTrcB_569_Fw and Inv_pTrcB_568_Rv. The atoB gene fragment was amplified by PCR using E. coli MG1655 genomic DNA as a template with the primer pair atoB_Fw and atoB_Rv. Both fragments were ligated, and the resulting plasmid was designated pMeESA. To construct the plasmid pMeAES, a similar procedure was carried out using the primer pairs Inv_pTrc-mvaE_Fw / Inv_pTrcB_412_Rv and atoB_pT_mvaES_Fw / atoB_pT_mvaES_Rv. The resulting plasmid was designated pMeAES. The plasmid pZA-AES was constructed as follows. The fragment atoB-mvaE-mvaS was amplified by PCR using pMeAES as a template with the primer pair pTrcHisB_Mev_Fw and pTrcHisB_Mev_Re. The fragment was cloned between the KpnI and HindIII sites of pZA23, and the resulting plasmid was designated pZA-AES. The blc-tfu0937 fragment was amplified by PCR using pHLA-blc-tfu0937 (Tanaka et al. 2011) as a template with the primer pair pTrcHisB-HCEpro-Fw and pTrcHisB-rrnbter-Rv. The linearized fragment was amplified by PCR using pMeASE as

a template with the primer pair Inv-pMeASE-Fw and Inv-pMeASE-Rv. Both fragments were ligated, and the resulting plasmid was designated pMeASE-BGL. The plasmid pTΔpgi was constructed as follows. The linearized fragment was amplified by PCR using pTargetF as a template with the primer pair pgi_N20inv_Fw and pgi_N20inv_Rv. The amplified fragment was self-ligated, and the resulting plasmid was designated pTΔpgiF. The upstream and downstream homologous DNA sequences of pgi were amplified using PCR using E. coli MG1655 genomic DNA as a template with the primer pairs pgi_HomSeq_Up_Fw / pgi_HomSeq_Up_Rv and pgi_HomSeq_Dw_Fw / pgi_HomSeq_Dw_Rv, respectively. Both amplified fragments were fused using overlap extension PCR with the primer pair pgi_HomSeq_Up_Fw and pgi_HomSeq_Dw_Rv. The amplified donor was cloned between the EcoRI and HindIII sites of pTΔpgiF, and the resulting plasmid was designated as pTΔpgi. The other plasmids of the pTarget series were constructed using the same procedures that were used to construct pTΔpgi.

Genetic deletions were carried out using the CRISPR-Cas2-plasmid system (Jiang et al. 2015). Plasmids pTΔpgi, pTΔpfkA, pTΔpfkB, pTΔgnd, pTΔaceBA, pTΔppc, and pTΔgltA were used to delete pgi, pfkA, pfkB, gnd, aceBA, ppc, and gltA, respectively.

2. Medium

M9Y medium was used for mevalonate production in 5 mL test tube-scale cultures. M9Y medium was comprised of M9 minimal medium supplemented with 0.5 % yeast extract, 0.008 g/L D-(+)-biotin, 0.2 g/L citrate, 0.008 g/L nicotinic acid, 0.032 g/L, pyridoxine and 1 mL/L trace metal solution. M9 minimal medium contains (per liter) 20 g glucose or cellobiose, 0.5 g NaCl, 6.7 g Na2HPO4, 3 g KH2PO4, 1 g NH4Cl, 246 mg MgSO4·7H2O, 14.7 mg CaCl2·2H2O, 2.78 mg FeSO4·7H2O, and 10 mg thiamine hydrochloride. When needed, ampicillin (100 mg/L) was added to the initial medium.

3. Culture Conditions

To promote mevalonate fermentation from glucose and cellobiose, metabolically-engineered strains were precultured in 5 mL LB medium overnight at 37 °C. The preculture medium was seeded to 5 mL M9Y medium in a 15 mL test tube at an initial optical density at 600 nm (OD600) of 0.05. After 3 h of cultivation, isopropyl β-D-1-thiogalactopyranoside was added to a final concentration of 0.1 mM. The tube-scale cultures were incubated at 37 °C with shaking at 220 rpm.

4. Analytical Methods

HCl (50 μL) was added to 300 μL of cultured cells and incubated at 60 °C with shaking

at 1000 rpm for lactonization. After 30 min, mevalonolactone was extracted with 350 μL of ethyl acetate containing beta-caryophyllene as an internal standard. Cell growth was determined by measuring the OD at 600 nm (OD600) on a UVmini-1240 spectrophotometer (Shimadzu Corporation, Kyoto, Japan). Extracted mevalonolactone was analyzed by gas chromatography (GC) using a GC-2025 chromatograph (Shimadzu Corporation, Kyoto, Japan) equipped with an SH-stabilwax (Length 30 m, Diameter 0.25 mm, Film 0.25 μm). Glucose and cellobiose were analyzed using a Prominence high-performance liquid chromatography (HPLC) System (Shimadzu Corporation, Kyoto, Japan) equipped with a Shodex SUGAR KS-801 column (6 μm, 300 mm × 8.0 mm, L × I.D., SHOWA DENKO, Tokyo, Japan).

Supplementary Table S1. Primers used in this study

plasmids	primers	gene order
pMeES	Inv_pTrcB_Fw	GATCCGAGCTCGAGATCTGCAGCT
	Inv_pTrcB_Rv	ACCATGATGATGATGATGAGAACC
pMeESA	Inv_pTrcB_569_Fw,	ATGAGAGAAGATTTTCAGCC
	Inv_pTrcB_568_Rv	CCGCCAAAACAGCCAAGCTT
	atoB_Fw	TGGCTGTTTTGGCGGaagagGTATATATTAatgaaaaattgtgtcatcgt
	atoB_Rv	AAAATCTTCTCTCATttaattcaaccgttcaatca
pMeAES	Inv_pTrc-mvaE_Fw	ATGAAAACCGTGGTGATTAT
	Inv_pTrcB_412_Rv	GGTTTATTCCTCCTTATTTA
	atoB_pT_mvaES_Fw	AAGGAGGAATAAACCatgaaaaattgtgtcatcgt
	atoB_pT_mvaES_Rv	CACCACGGTTTTcatTAATATATACctcttTAAttaattcaaccgttcaatca
pMeAES-BGL	pTrcHIsB-inv-Fw	AGTAGGACAAATCCGCCGGGAGCGGATTTG
	pTrcHisB-inv-Rv	CAGGAGAGCGTTCACCGACAAACAACAGATAAAACG
	pTrcHisB-HCEpro-Fw	GTGAACGCTCTCCTGgctagcttgatctctccttcacagattcccaatctcttg
	pTrcHisB-rrnbter-Rv	CGGATTTGTCCTACTttgtagaaacgcaaaaaggccatccgtcagg
pZA-AES	pTrcHisB_Mev_Fw	TTAAAGAGGAGAAAGGTACCATGAAAAATTGTGTCATCGTCAGTGCGGTACG
	pTrcHisB_Mev_Re	ATTCGATATCAAGCTttaATTACGATAGCTACGCACGGTGTTATTAATGGCG
pTΔpgi	pgi_N20inv.Fw	GTCACCATGTATGGGCCGGGTTTTAGAGCTAGAAATAGCAAGTTAAAATAAGGC
	pgi_N20inv.Rv	GCCCATACATGGTGACCGGCTAGCATTATACCTAGGACTGAGCTAGCTGTCAAGG
	pgi_HomSeq_Up_Fw	TGCTTTTTTTGAATTGGCCTGCGCTAGCGCAGGTAGTAC

	pgi_HomSeq_Up_Rv	CTTTCAGGAACCAGTCACGTTACGCAGCGCTACGTGCAGCAC
	pgi_HomSeq_Dw_Fw	CGTAGCGCTGCGTAACGTGACTGGTTCCTGAAAGCGGCAG
	pgi_HomSeq_Dw_Rv	GCTTCTGCAGGTCGACGACAGCAGTTTCTGGTGATGATCAGAGAGC
	pfkA_N20inv_Fw	GTCTGACATGATCAACCGGGTTTTAGAGCTAGAAATAGCAAGTTAAAATAAGGC
	pfkA_N20inv_Rv	GTTGATCATGTCAGACACGCTAGCATTATACCTAGGACTGAGCTAGCTGTCAAGG
pTΔpfkA	pfkA_HomSeq_Up_Fw	TGCTTTTTTTGAATTCGTACAGTCATTACTGGATCGCGCATTGC
	pfkA_HomSeq_Up_Rv	CATGTAGGAACCGTCACCTGTTGCCGGAAGTCTTCTTGCACATCG
	pfkA_HomSeq_Dw_Fw	GACTTCCGGCAACAGGTGACGGTTCCTACATGGGTGCAATG
	pfkA_HomSeq_Dw_Rv	GCTTCTGCAGGTCGACTACGGTCGTAAGGCACCGGAGAACCAC
	pfkB_N20inv_Fw	ACCGGTGTTCGAACCCGGGGTTTTAGAGCTAGAAATAGCAAGTTAAAATAAGGC
	pfkB_N20inv_Rv	GGGTTCGAACACCGGTGCGCTAGCATTATACCTAGGACTGAGCTAGCTGTCAAGG
pTΔpfkB	pfkB_HomSeq_Up_Fw	TGCTTTTTTTGAATTCGATGAAGCTGATGTGATTGCGCAAGC
	pfkB_HomSeq_Up_Rv	GCTTCTGCAGGTCGACGATTTTCCTGCTCAAACACCTTCAACACTTC
	pfkB_HomSeq_Dw_Fw	CTGCTTCCAGGTGCTGCACGGCATAAGCGAGGATGACG
	pfkB_HomSeq_Dw_Rv	GCTTCTGCAGGTCGACGATTTTCCTGCTCAAACACCTTCAACACTTC
	gnd_N20inv_Fw	AATGGTGAAAGCAGGTGCGGTTTTAGAGCTAGAAATAGCAAGTTAAAATAAGGC
	gnd_N20inv_Rv	ACCTGCTTTCACCATTAAGCTAGCATTATACCTAGGACTGAGCTAGCTGTCAAGG
pTΔgnd	gnd_HomSeq_Up_Fw	TGCTTTTTTTGAATTCGGTGCGCAGGATCATTTATGCTGGTACG
	gnd_HomSeq_Up_Rv	GGCTTCTTTCTGGCCACACCACGGCTTTCGATGTTGAGCG
	gnd_HomSeq_Dw_Fw	CGAAAGCCGTGGTGTGGCCAGAAAGAAGCCTATGAATTGGTAGCAC
	gnd_HomSeq_Dw_Rv	GCTTCTGCAGGTCGACACGCAGCACGCAGCTGAGAGAAGC
pTΔaceBA	aceBA_N20inv_Fw	TGGCATCGCAGCAATCCGGGTTTTAGAGCTAGAAATAGCAAGTTAAAATAAGGC

	aceBA_N20inv_Rv	GATTGCTGCGATGCCACTGCTAGCATTATACCTAGGACTGAGCTAGCTGTCAAGG
	aceBA_HomSeq_Up_Fw	TGCTTTTTTTGAATTGTAGAGCGCAAGATGGTGATCAACGCG
	aceBA_HomSeq_Up_Rv	GAAGTAATCGACATAGCGCGGTTTATCCATCGTCACTGCCTGTCTGTC
	aceBA_HomSeq_Dw_Fw	CGATGGATAAACCGCGCTATGTCGATTACTTCCTGCCGATC
	aceBA_HomSeq_Dw_Rv	GCTTCTGCAGGTCGACCGAGGTTTTTCTGCCAGTTGAACGACG
	ppc_N20inv_Fw	GGCGGCAATGGAGCCTTGGGTTTTAGAGCTAGAAATAGCAAGTTAAAATAAGGC
	ppc_N20_inv_Rv	AGGCTCCATTGCCGCCTAGCTAGCATTATACCTAGGACTGAGCTAGCTGTCAAGG
pTΔppc	ppc_HomSeq_Up_Fw	TGCTTTTTTTGAATTCACCCCTGAACTGCTGGCGCTGG
	ppc_HomSeq_Up_Rv	CGCTATCCATCGAAGATGGATGTGTGTTGTTGCGGTGCTTCGGCAATCAC
	ppc_HomSeq_Dw_Fw	GCAAGTAAAACCTCTACAAATGTGGTATTGGCGGCTCCATTGCCGCCTACGTG
	ppc_HomSeq_Dw_Rv	GCTTCTGCAGGTCGACGTAGCGGAGCGGAAGTAAGGCAC
	gltA_N20inv_Fw	CGATTCTGGAACGTGCTAgttttagagctagaaatagcaagttaaaataaggctagtccg
	gltA_N20inv_Rv	CACGTTCCAGAATCGGAactCgtattatacctaggactgagctagctgtcaaggatccag
pTΔgltA	gltA_HomSeq_Up_Fw	tgctttttttgaattcAGTCGCGTTTTTCATATCCTGTATACAGCTG
	gltA_HomSeq_Up_Rv	GGATGTTAACAAactagtCGGAATTTGTTCGTCGTGCG
	gltA_HomSeq_Dw_Fw	CGAACAAATTCCGactagtTTGTTAACATCCAGCGAGTCGTGATAGA
	gltA_HomSeq_Dw_Rv	aatagatctaagcttaTGTGCTGAAAGGCACGCTGG

Supplementary Table S2. Sequence of synthesized genes used in this study

mvaS	ATCTGCAGCTGGTACAAAATTAaagagGTATATATTAatgACCATTGGCATCGACAAGATCAGCTTTTTTGTTCCGCCTT
	ATTACATCGATATGACCGCACTGGCCGAAGCACGTAATGTTGATCCGGGTAAATTTCATATTGGTATTGGTCAGGA

TCAGATGGCCGTTAATCCGATTAGCCAGGATATTGTTACCTTTGCAGCAAATGCAGCAGAAGCAATTCTGACCAAA
GAAGATAAAGAAGCGATCGATATGGTTATTGTTGGCACCGAAAGCAGCATTGATGAAAGCAAAGCAGCCGCAGTTG
TTCTGCATCGTCTGATGGGTATTCAGCCGTTTGCACGTAGCTTTGAAATTAAAGAAGCATGTTACGGCGCAACCGC
AGGTCTGCAGCTGGCAAAAAATCATGTTGCACTGCATCCGGATAAAAAAGTTCTGGTTGTTGCAGCAGATATCGCC
AAATATGGTCTGAATAGCGGTGGTGAACCGACACAAGGTGCCGGTGCAGTTGCAATGCTGGTTGCAAGCGAACCG
CGTATTCTGGCACTGAAAGAGGATAATGTTATGCTGACGCAGGATATCTATGATTTTTGGCGTCCGACCGGTCATC
CGTATCCGATGGTTGATGGTCCGCTGAGCAATGAAACCTATATTCAGAGCTTTGCACAGGTGTGGGATGAACATAA
AAAACGTACCGGTCTGGATTTCGCAGATTATGATGCACTGGCCTTTCATATTCCGTATACCAAAATGGGTAAAAAAG
CACTGCTGGCCAAAATTAGCGATCAGACCGAAGCCGAACAAGAACGTATCCTGGCACGTTATGAAGAAAGCATTATC
TATAGCCGTCGTGTGGGTAATCTGTATACCGGTAGCCTGTATCTGGGTCTGATTAGCCTGCTGGAAAATGCAACCA
CACTGACCGCTGGTAATCAGATTGGTCTGTTTAGCTATGGTAGCGGTGCCGTTGCAGAATTCTTTACCGGTGAACT
GGTTGCAGGTTATCAGAATCATCTGCAGAAAGAAACCCATCTGGCCCTGCTGGATAATCGTACCGAACTGAGCATT
GCAGAATATGAAGCAATGTTTGCAGAAACCCTGGATACCGATATTGATCAGACCCTGGAAGATGAACTGAAATATAG
CATTAGCGCCATTAATAACACCGTGCGTAGCTATCGTAATtaaGTACCATATGGGAAT

mvaE catcatcatcatggtATGAAAACCGTGGTGATTATTGATGCACTGCGTACCCCGATTGGTAAATACAAAGGTAGCCTGAGCCAGGT
TAGCGCAGTTGATCTGGGCACCCATGTTACCACACAGCTGCTGAAACGTCATAGCACCATTAGCGAAGAAATTGATCAGG
TGATTTTTGGCAATGTTCTGCAGGCAGGTAATGGTCAGAATCCGGCACGTCAGATTGCAATTAATAGCGGTCTGAGCCAT
GAAATTCCGGCAATGACCGTTAATGAAGTTTGTGGTAGCGGTATGAAAGCAGTTATTCTGGCAAAACAGCTGATCCAGCT
GGGTGAAGCCGAAGTTCTGATTGCCGGTGGTATTGAAAATATGAGCCAGGCACCGAAACTGCAGCGTTTCAATTATGAAA
CCGAAAGCTATGATGCACCGTTTAGCAGCATGATGTATGATGGTCTGACCGATGCATTTAGCGGTCAGGCAATGGGTCT
GACAGCAGAAAATGTTGCAGAAAAATATCATGTGACCCGTGAAGAACAGGATCAGTTTAGCGTTCATAGCCAGCTGAAAG
CAGCACAGGCACAGGCCGAAGGTATTTTTGCAGATGAAATTGCACCGCTGGAAGTTAGCGGCACCCTGGTTGAAAAAGAT
GAAGGTATTCGTCCGAATAGCAGCGTTGAAAAACTGGGTACACTGAAAACGGTGTTTAAAGAAGATGGCACCGTTACCGC

AGGCAATGCAAGTACCATTAATGATGGTGCAAGCGCACTGATTATTGCCAGCCAAGAATATGCCGAAGCACATGGTCTGC
CGTATCTGGCAATTATTCGTGATAGCGTTGAAGTTGGTATTGATCCGGCATATATGGGTATTAGCCCGATTAAAGCAATT
CAGAAACTGCTGGCACGTAATCAGCTGACCACCGAAGAAATCGACCTGTATGAAATTAATGAAGCATTTGCCGCAACCAG
CATTGTTGTTCAGCGTGAACTGGCACTGCCGGAAGAAAAAGTTAACATTTATGGTGGTGGTATCAGCCTGGGTCATGCAA
TTGGTGCAACCGGTGCACGTCTGCTGACCAGCCTGAGCTATCAGCTGAATCAGAAAGAAAAAAAGTATGGTGTTGCCAGC
CTGTGTATTGGTGGTGGCCTGGGTTTAGCAATGCTGCTGGAACGCCCTCAGCAGAAGAAAAATAGCCGTTTTTATCAGAT
GAGTCCGGAAGAACGTCTGGCAAGCCTGCTGAATGAAGGTCAGATTAGCGCAGATACCAAAAAAGAATTTGAAAACACCG
CACTGAGCAGCCAGATTGCCAACCATATGATTGAAAATCAGATCAGCGAAACCGAAGTTCCGATGGGTGTTGGTCTGCAT
CTGACCGTGGATGAAACGGATTATCTGGTGCCGATGGCAACCGAAGAACCGAGCGTTATTGCAGCCCTGAGCAATGGTG
CAAAAATTGCACAGGGCTTTAAAACCGTGAATCAGCAGCGTCTGATGCGTGGTCAGATTGTTTTTTATGATGTTGCCGAT
GCAGAAAGCCTGATTGATGAACTGCAGGTTCGTGAAACAGAAATTTTCCAGCAGGCAGAACTGAGTTATCCGAGCATTGT
TAAACGCGGTGGTGGTCTGCGTGATCTGCAGTATCGTGCATTTGATGAAAGCTTTGTTAGCGTGGATTTTCTGGTGGAT
GTTAAAGATGCAATGGGTGCCAATATTGTTAATGCAATGCTGGAAGGTGTTGCCGAACTGTTTCGTGAATGGTTTGCAGA
ACAGAAGATTCTGTTTAGCATCCTGAGTAATTATGCCACCGAAAGTGTTGTTACCATGAAAACAGCAATTCCGGTTAGCC
GTCTGAGCAAAGGTAGTAATGGTCGTGAAATTGCCGAAAAAATTGTTCTGGCCAGCCGTTATGCAAGCCTGGATCCGTAT
CGTGCGGTTACCCATAATAAAGGTATTATGAATGGCATTGAAGCAGTTGTGCTGGCCACCGGTAATGATACCCGTGCAGT
TAGCGCAAGCTGTCATGCATTTGCAGTTAAAGAAGGTCGTTATCAGGGTCTGACCAGCTGGACCCTGGATGGTGAGCAG
CTGATTGGTGAAATTAGCGTTCCGCTGGCACTGGCAACCGTTGGTGGTGCCACCAAAGTTCTGCCGAAAAGCCAGGCAG
CAGCCGATCTGCTGGCAGTTACCGATGCAAAAGAACTGAGCCGTGTTGTTGCAGCAGTTGGTCTGGCACAGAATCTGGC
AGCACTGCGTGCACTGGTTAGCGAAGGCATTCAGAAAGGTCATATGGCACTGCAGGCACGTTCACTGGCCATGACCGTG
GGTGCGACCGGTAAAGAAGTTGAAGCCGTTGCGCAGCAGTTAAAACGTCAGAAAACAATGAATCAGGATCGTGCCCTGGC
AATTCTGAATGATCTGCGTAAACAGtaaGATCCGAGCTCGAGA